



CONTRACT NO. 93-310
FINAL REPORT
MAY 1996

Impact of Improved Emissions Characterization for Nitrogen-Containing Air Pollutants for the South Coast Air Basin

TD
883.1
H3
1996



CALIFORNIA ENVIRONMENTAL PROTECTION AGENCY
AIR RESOURCES BOARD
Research Division

**Impact of Improved Emissions Characterization
for Nitrogen-Containing Air Pollutants
for the South Coast Air Basin**

Final Report

Contract No. 93-310

Prepared for:

**California Air Resources Board
Research Division
2020 L Street
Sacramento, CA 95814**

Prepared by:

**Robert A. Harley
Principal Investigator**

**Department of Civil and Environmental Engineering
University of California
Berkeley, CA 94720-1710**

May 1996

Disclaimer

The statements and conclusions in this report are those of the principal investigator and not necessarily those of the California Air Resources Board. The mention of commercial products, their source, or their use in connection with material reported herein is not to be construed as actual or implied endorsement of such products.

Acknowledgments

The principal investigator acknowledges the assistance of Nancy Brown of Lawrence Berkeley Laboratory, Ted Russell of Carnegie Mellon University, and Tom Kirchstetter of UC Berkeley. Technical support was provided by Randy Pasek and Bart Croes of the California Air Resources Board throughout the course of this project. Helpful comments and data related to the SCAQS sampler were provided by Susanne Hering of Aerosol Dynamics Inc., and Fred Lurmann of Sonoma Technology Inc.

This report was submitted in fulfillment of Inter-Agency agreement number 93-310 by the University of California at Berkeley, under the sponsorship of the California Air Resources Board. Work was completed as of December 20, 1995.

Abstract

Nitrogen-containing air pollutants contribute to many of California's air quality problems. The impact of improved characterization of emissions of oxides of nitrogen and ammonia was studied using the CIT airshed model applied to the August 27–29, 1987, intensive monitoring period from the Southern California Air Quality Study. Direct NO_2 and nitrous acid emissions at levels between 0–10% and 0–3%, respectively, were used to examine the influence of NO_x emission speciation. A 50% reduction in total NO_x mass emissions was used to compare the importance of mass emissions and emission speciation. A new NH_3 emission inventory developed for the South Coast Air Basin was used in this study.

Model predictions matched the spatial and temporal distribution of observed concentrations of O_3 , NO_2 , PAN, HNO_3 , and fine particle nitrate. Predicted pollutant concentrations were much more sensitive to NO_x mass emissions than to NO_x speciation. Daytime NO_2 concentrations were governed by the rate of conversion of NO to NO_2 in the atmosphere, not by direct NO_2 emissions. Nighttime NO_2 and nitrous acid concentrations were sensitive to NO_x speciation. Reducing NO_x emissions led to significant reductions in concentrations of NO_2 , nitric acid, and fine particle nitrate, whereas predicted ozone and PAN concentrations increased.

Direct emissions of NO_2 and nitrous acid appear to be at the low end (i.e., close to zero) of the ranges studied here. Heterogeneous conversion of

NO_x is likely to be the main source of nitrous acid in the atmosphere.

To support modeling and control strategy development for nitrogenous air pollutants, improvements are needed to the ammonia emission inventory. Continuing shifts in agricultural activities within the South Coast Air Basin need to be tracked, the diurnal variation profiles for ammonia emissions need to be improved, and new measurements of ammonia emissions from cattle and poultry farms are needed.

Contents

1	Introduction	1
2	Approach	10
3	Application	14
3.1	Southern California Air Quality Study	14
3.2	Emission Inventory	15
3.3	Observed Pollutant Concentrations	18
4	Results	21
5	Discussion	28
6	Conclusions	32
7	Recommendations	33
8	References	34
A	Time Series Plots	39
B	Concentration Isopleth Plots	58

1 Introduction

Nitrogen-containing air pollutants, especially the oxides of nitrogen (NO_x), play a central role in many of California's current air quality problems. Reductions in emissions of volatile organic compounds (VOC) have helped to reduce ambient ozone concentrations in California, but NO_x emission reductions will be needed to help solve the State's remaining ozone, acid deposition, visibility, and PM_{10} problems. In addition to understanding and controlling total pollutant mass emission rates, the detailed chemical composition of the emissions also is important, as shown for the case of VOC emissions by Harley et al. (1992).

While most of the direct NO_x emissions are in the form of nitric oxide (NO), other important nitrogen-containing pollutants that are directly emitted include nitrogen dioxide (NO_2), nitrous acid (HONO), and nitrous oxide (N_2O). Nitrogen dioxide is one of six criteria pollutants for which National Ambient Air Quality Standards have been established. NO_2 in combustion system exhaust can lead to plume discoloration problems for large point sources. Nitrous acid photolyzes in the atmosphere to produce hydroxyl radicals which in turn initiate photochemical smog reactions. Nitrous oxide has been identified as a greenhouse gas and a scavenger of stratospheric ozone, and is therefore of concern even though it is unreactive in the troposphere. Ammonia (NH_3) is another important nitrogen-containing air pollutant, although combustion is a minor source of ammonia compared to waste decom-

position sources. Ammonia reacts with nitric acid in the atmosphere to form ammonium nitrate, a condensable product which contributes to particulate matter concentrations.

At present, emission inventories used in photochemical modeling studies generally assume that NO_x emissions are uniformly composed of 95% nitric oxide, 5% nitrogen dioxide, and 0.5% nitrous acid regardless of the source type.

Research Objectives

The objectives of this research are to: (1) study the sensitivity of predicted air pollutant concentrations to changes in the direct emission rates of NO_2 and HONO; and (2) compare predicted and observed concentrations of nitrogen-containing air pollutants for the August 27-29, 1987 intensive monitoring period from the Southern California Air Quality Study (SCAQS).

NO_x Emissions

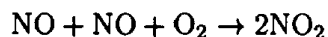
While the majority of direct NO_x emissions are in the form of NO, other pollutants including NO_2 , N_2O , and HONO are also emitted. A review of prior studies of the direct emissions of these pollutants is presented below.

Nitrogen Dioxide

Nitrogen dioxide (NO_2) can be formed during combustion (Heywood, 1988) when exhaust gases cool rapidly, allowing high concentrations of hydroperoxyl radical (HO_2^*) to persist, and resulting in conversion of NO to NO_2 by the reaction:



In addition to NO₂ formation in combustion, some NO may be oxidized to NO₂ in the exhaust plume from a combustion source while NO concentrations remain high:



Because of the way motor vehicle emission standards have been specified, most measurements of motor vehicle exhaust NO_x emissions report only total NO_x, without any subdivision of the total into individual species. However, in selected studies, more detailed measurements have been made (Cadle et al., 1979; Hilliard and Wheeler, 1979; Lenner et al., 1983; Lenner, 1987). Early measurements suggested average NO₂ fractions of 12% for engine-out emissions, with tailpipe-out NO₂ fractions of 5% (Cadle et al., 1979). High ambient NO₂ concentrations measured during the winter in Sweden led to measurements of the NO₂ fraction in gasoline engine exhaust at low temperatures and at various engine loads (Lenner et al., 1983; Lenner, 1987). NO₂ fractions of up to 50% were measured in warmed up engines operating at idle or low load conditions (Lenner, 1987). The NO₂ fraction tended to decrease as engine load increased, whereas total NO_x emissions increased with increasing engine load. The nature of the emission control systems installed on the vehicle also affected NO_x speciation significantly: the highest NO₂ fractions were measured in a vehicle equipped with an air injection (pulsair) system and in a vehicle equipped with a thermal reactor designed to oxidize hydrocarbons and carbon monoxide in the exhaust. The lowest NO₂ fractions were measured in a vehicle equipped with a three-way catalyst system (Lenner, 1987). Recent measurements made during the Auto/Oil study confirm that NO₂ fractions are very low (1.3% of total NO_x) in normal-emitting vehicles equipped with three-way catalyst systems (Sawyer, 1992).

NO₂ has been measured in diesel engine exhaust by several investigators (Harris, 1987; Lenner, 1987). A passenger diesel vehicle equipped with EGR had measured NO₂ fractions in the range 15-35% (Lenner, 1987). NO₂ concentrations measured by Harris (1987) decreased with increasing engine load, consistent with previous findings for gasoline-powered vehicles.

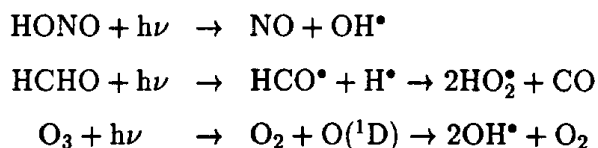
Gas turbines are used in electric power generation, and a study by Johnson and Smith (1978) indicated high NO₂ fractions in the NO_x emissions from a 150 MW gas turbine power station. All of the NO_x emitted at idle was in the form of NO₂; even at full load the NO₂ fraction was 22%. Spectroscopic measurements of the NO₂ flux in the power plant plume were consistent with the direct stack sampling results. Therefore, power plants using gas turbines may be a significant source of direct NO₂ emissions in California.

Nitrous Acid

Nitrous acid has been measured in motor vehicle exhaust by Pitts et al. (1984). Nitrous acid has been detected in indoor air; both direct emissions and conversion of NO₂ have been identified as contributors (Pitts et al., 1985; Pitts et al., 1989). Measurements of nitrous acid in outdoor air have been reported by several investigators (Harris et al., 1982; Sjödin, 1988; Vecera and Dasgupta, 1991; Winer and Biermann, 1994). The diurnal pattern of measured nitrous acid concentrations shows a buildup overnight attributed both to direct emissions and in situ atmospheric formation, and rapid photolysis of HONO during daylight hours. Croes (1991) has reviewed the available source and ambient measurements of nitrous acid, and has recommended that until better information becomes available, nitrous acid emissions at the level of 2% of total NO_x should be used; sensitivity studies to investigate alternative

scenarios of 1 and 3% HONO were also recommended.

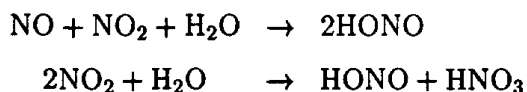
Nitrous acid is a significant atmospheric pollutant because it forms hydroxyl radicals as one of its photodissociation products. The hydroxyl radical is important in photochemical smog formation (for a detailed discussion, see Finlayson-Pitts and Pitts, 1986). The major photochemical reaction-initiating steps include photolysis of nitrous acid, formaldehyde (HCHO) and ozone:



During the 1987 Southern California Air Quality Study, Winer and Biermann (1994) measured nitrous acid, NO_2 , and formaldehyde concentrations at the Long Beach and Claremont air monitoring sites using differential optical absorption spectroscopy (DOAS). Significant diurnal variation in nitrous acid levels was noted, with very low concentrations observed during the daytime, and a buildup of nitrous acid overnight. The highest concentrations (up to 13.5 ppb) were observed at Long Beach during the fall. Using measured concentrations of nitrous acid, formaldehyde, and ozone, Winer and Biermann calculated radical generation rates from the photolysis of the measured species. It was found that for monitoring periods in November and December of 1987, nitrous acid photolysis was the dominant source of hydroxyl radicals during the early morning hours after sunrise.

Winer and Biermann also estimated contributions to ambient HONO concentrations due to direct nitrous acid emissions and in situ conversion of NO_2 in the atmosphere. Their data from Long Beach in the fall of 1987 suggest a nitrous acid fraction of 0.8% in direct NO_x emissions and a pseudo-first

order rate constant for NO₂ conversion of 1.0% per hour. The heterogeneous mechanism by which NO₂ is converted to nitrous acid in the atmosphere is not completely understood, although reactions such as:



have been reviewed (Calvert et al., 1994).

Measurements of nitrous acid emissions from motor vehicles traveling through the Caldecott tunnel (Kirchstetter et al., 1996) indicate that direct HONO emissions from motor vehicles are low. The measured HONO to NO_x ratio for uphill traffic at the Caldecott tunnel was $(2.9 \pm 0.5) \times 10^{-3}$. These measurements suggest that ambient HONO concentrations are governed mainly by heterogeneous formation.

Nitrous Oxide

Early suggestions that coal and fuel oil combustion were significant sources of N₂O emissions have now been discounted because even brief delays in analyzing stack gas samples containing SO₂ and NO_x can result in a significant N₂O sampling artifact (Muzio and Kramlich, 1988; Muzio et al., 1989). With respect to motor vehicle emissions, there is nevertheless concern that three-way catalytic converters may be converting some NO to N₂O instead of completely reducing NO to N₂. Dynamometer measurements of emissions from 32 vehicles indicated N₂O emission rates of 3.6 mg/mile from noncatalyst cars versus 45 mg/mile for cars equipped with three-way catalyst systems (Dasch, 1992). Additional measurements of motor vehicle N₂O emissions have been reported in European tunnel studies (Berges et al., 1993; Sjödin et al., 1994). The global impact of N₂O emissions is beyond the scope of this

study; N₂O does not contribute significantly to formation of photochemical smog in urban atmospheres.

Ammonia

An ammonia emission inventory for the South Coast Air Basin was prepared by Gharib and Cass (1984). A calculated total of 165×10^3 kg/day of ammonia was emitted to the air basin in 1982. The dominant sources of ammonia emissions in 1982 were livestock (52%), domestic pets such as dogs and cats (9%), flux from soils (14%), and sewage treatment plants (9%). Combustion sources such as motor vehicles and power plants were not significant sources of ammonia. Dickson (1991) has prepared an updated ammonia emission inventory for 1987 using data from Gharib and Cass (1984) together with updated activity and emission factor data. Between 1982 and 1987, many cattle feedlots and dairies relocated outside the air basin, whereas poultry farming within the air basin increased (Dickson, 1991). More recent measurements in the South Coast Air Basin suggest that emissions from dairy farms may be overstated in current ammonia emission inventories (Schmidt and Winegar, 1996).

Emissions of ammonia from motor vehicles were predicted to increase between 1982 and 1987 because of the increased use of three-way catalytic converters, and the associated increase in emissions of reduced nitrogen species such as ammonia. Nevertheless, motor vehicle exhaust still contributes only a minor fraction (3%) of total ammonia emissions in the air basin. A summary of the 1987 ammonia emission inventory is presented below in Table 1; the spatial distribution of ammonia emissions is plotted in Figure 1.

Table 1: Summary of ammonia emission inventory
 South Coast Air Basin, 1987 (from Dickson, 1991)

source	NH ₃ emissions (10 ³ kg/day)	percent of total
soil surface	35.0	16.4%
fertilizer application		3.5%
farm crops	3.0	
orchards & ornamental	0.6	
anhydrous ammonia	0.2	
non-farm	3.7	
livestock waste		45.1%
cattle - dairy	26.9	
cattle - feedlot	0.3	
cattle - range	14.3	
horses	8.9	
sheep	0.2	
hogs	0.2	
chickens - layers	35.5	
chickens - fryers	2.2	
chickens - pullets	7.3	
turkeys	0.6	
domestic emissions		11.8%
dogs	10.9	
cats	2.4	
human respiration	0.1	
human perspiration	8.6	
household ammonia use	0.6	
untreated human waste	2.3	
cigarette smoke	0.3	
fuel combustion	0.6	0.3%
on-road vehicles	6.4	3.0%
point sources	42.5	19.9%
grand total	214	

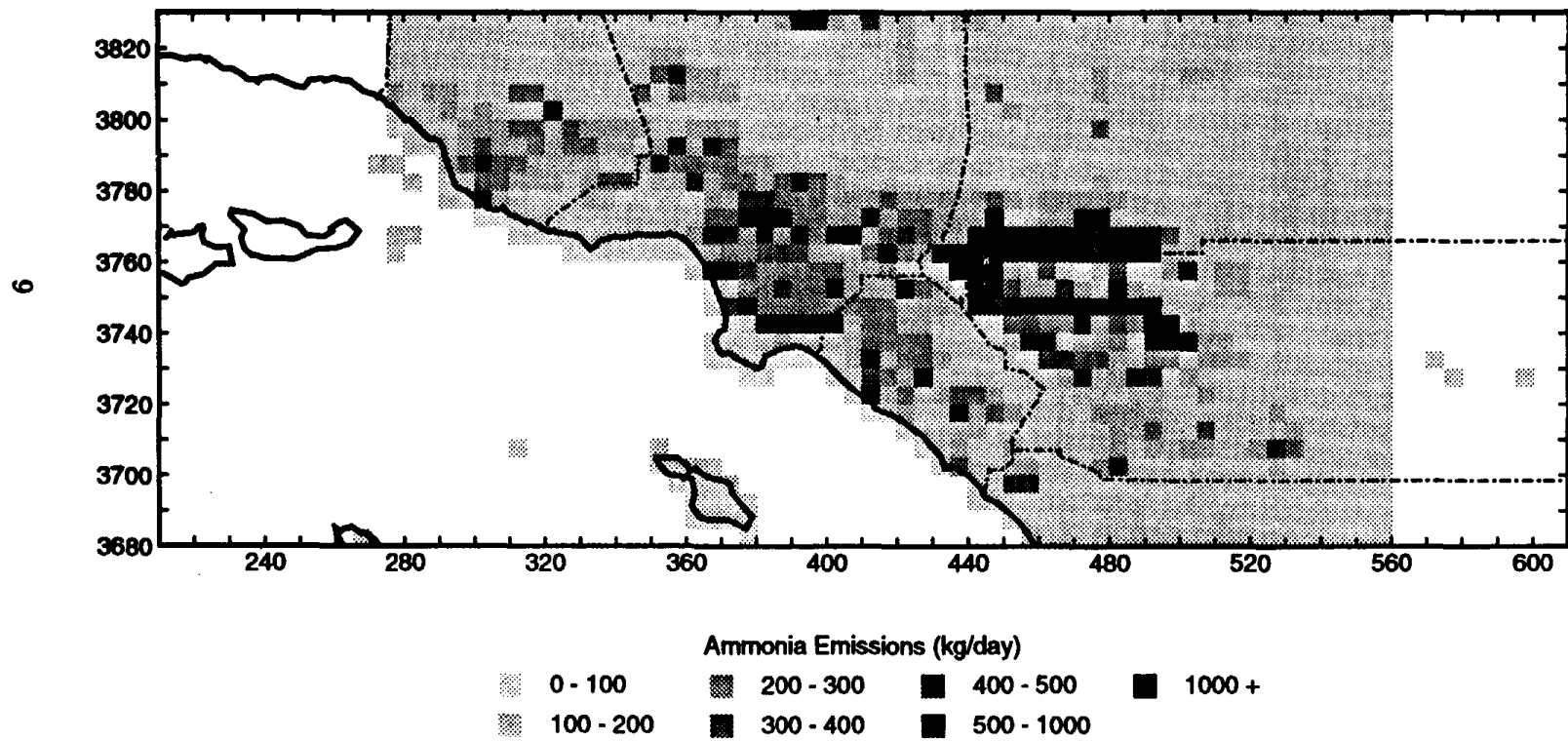


Figure 1. Spatial distribution of ammonia emissions in the South Coast air basin, August 1987.

2 Approach

The transport and photochemical transformation of air pollutant emissions within the South Coast air basin were studied using a three-dimensional Eulerian air quality model (McRae et al., 1982; Russell et al., 1988; Harley et al., 1993a). This model, referred to as the CIT airshed model, solves the atmospheric diffusion equation numerically for the concentration C_i of pollutant species i :

$$\frac{\partial C_i}{\partial t} + \nabla \cdot (\vec{u}C_i) = \nabla \cdot (K\nabla C_i) + R_i + Q_i$$

where the equation is solved simultaneously for multiple chemical species ($i=1,2,3, \dots n$). The equations are coupled via second-order chemical reactions. The terms in the above equation are defined as follows: \vec{u} is the wind velocity vector, K is the eddy diffusivity tensor, R_i is the net rate of generation of species i by chemical reactions, and Q_i is the rate of direct emissions from elevated chimney stacks. Ground-level emissions are accounted for in the surface boundary condition:

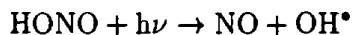
$$-K_{zz} \frac{\partial C_i}{\partial z} = E_i - v_g^i C_i$$

where E_i is the upward flux of direct pollutant species i emissions, and v_g^i is the dry deposition velocity for species i . Lateral boundary conditions and initial conditions were specified using measured pollutant concentration data. At the top of the modeling region, a zero concentration gradient condition

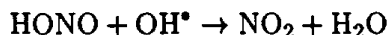
was applied, so that the model predictions in the highest computational layer were used to estimate pollutant concentrations above the modeling region.

Gas-phase photochemical reactions were represented within the model using the LCC surrogate species chemical mechanism (Lurmann et al., 1987). The mechanism includes 35 active chemical species and 107 reactions. Hydrocarbons are lumped together into 5 different species groups: C₄ and larger alkanes, ethene, C₃ and larger alkenes, monoalkyl benzenes (e.g., toluene), and di- and trialkyl benzenes (e.g., xylene and trimethylbenzene). Additional organic species tracked in the mechanism include formaldehyde, acetaldehyde, and methyl ethyl ketone. The latter two species are used as surrogate species for all C₂ and higher aldehydes, and all ketones, respectively. The published version of the LCC mechanism was extended to include as explicit species sulfur dioxide, isoprene, methanol, ethanol, methyl tert-butyl ether, and methane, as described in more detail by Harley et al. (1993a).

Several nitrous acid reactions are included in the LCC mechanism. The most important sink for nitrous acid during the daytime is photolysis:

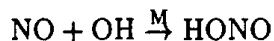


The rate constant depends on sunlight intensity, but for overhead sun, $J = 0.098 \text{ min}^{-1}$ in the LCC mechanism. The Carbon Bond IV mechanism (CB4; Gery et al., 1989) includes another sink for nitrous acid:

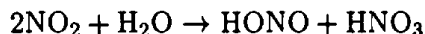


with a rate constant of $6.6 \times 10^{-12} \text{ cm}^3 \text{ molecule}^{-1} \text{ s}^{-1}$. Although this HONO sink is not included in the LCC mechanism, Calvert et al. (1994) state that photolysis is the dominant sink for nitrous acid, and that the

reaction of HONO with the hydroxyl radical represents only a few percent of total HONO removal. Both LCC and CB4 mechanisms include a three-body reaction forming nitrous acid:

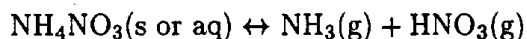


The pseudo-second order rate constant for this reaction in the LCC mechanism is $4.0 \times 10^{-13} \exp(833/T) \text{ cm}^3 \text{ molecule}^{-1} \text{ s}^{-1}$. The reaction of NO with hydroxyl radicals to form nitrous acid does not explain the observed buildup of nitrous acid concentrations overnight, when hydroxyl radical concentrations are low. The LCC mechanism includes one additional reaction forming HONO:



with a pseudo-second order rate constant $k = 4.0 \times 10^{-24} \text{ cm}^3 \text{ molecule}^{-1} \text{ s}^{-1}$, and a rate expression of $k[\text{NO}_2][\text{H}_2\text{O}]$. The CB4 mechanism forms nitrous acid by the reaction of $\text{NO} + \text{NO}_2 + \text{H}_2\text{O}$ instead (Gery et al., 1989).

Ammonium nitrate formation and transport are tracked in the model using the method described by Russell et al. (1983) which assumes equilibrium among gas-phase ammonia, gas-phase nitric acid, and particulate ammonium nitrate in the solid or aqueous phase:



The equilibrium constant is calculated for the above reaction using equations developed by Stelson and Seinfeld (1982ab) as a function of temperature and relative humidity. The equilibrium assumption has been evaluated against field observations (e.g., Hildemann et al., 1984; Harrison and Msibi, 1994). Wexler and Seinfeld (1990) found that in some cases during SCAQS, departures from equilibrium were observed. Wexler et al. (1994) have developed a

different modeling approach for urban and regional aerosols that represents the kinetics as well as the thermodynamics of aerosol formation. However, since uncertainties in the emission rates of ammonia, NO_x , and VOC are likely to dominate the problem of modeling ammonium nitrate formation, the equilibrium assumption has been used in the present study.

3 Application

3.1 Southern California Air Quality Study

During the summer and fall of 1987, a comprehensive set of meteorological and air pollutant measurements were made as part of the Southern California Air Quality Study or SCAQS (Lawson, 1990). Special measurements made during SCAQS include: upper air soundings for vertical temperature, humidity, and wind profiles; chemically speciated $PM_{2.5}$ and PM_{10} concentrations; and speciated hydrocarbon and carbonyl concentrations. Numerous other special study measurements were made at the Claremont and Long Beach monitoring sites, as described in more detail by Lawson (1990) and references therein. A map showing the network of special SCAQS monitoring sites is presented in Figure 2.

The CIT airshed model was applied to the August 27-29, 1987, SCAQS intensive monitoring period over the computational domain shown in Figure 2. Initial conditions and lateral inflow boundary conditions were specified using measured pollutant concentrations, as described by Harley et al. (1993a). The same meteorological fields developed and used as part of a previous photochemical modeling study of the August SCAQS episode (Harley et al., 1993ab) were used in this study.

3.2 Emission Inventory

The baseline emission inventory used in the present study was obtained from the California Air Resources Board (Wagner and Allen, 1990). The inventory includes stationary point source and area source emission estimates, as well as on-road motor vehicle emissions estimated using California's EMFAC 7E model. Stabilized hot exhaust emissions of CO and VOC from motor vehicles were scaled up to three times the baseline (EMFAC 7E) values, consistent with measurements of on-road vehicle emissions in the Sherman Way tunnel in Van Nuys, CA (Ingalls et al., 1989; Pierson et al., 1990). Revised VOC speciation profiles developed by Harley et al. (1992) were used in this study. NO_x emissions were assumed to consist of 93% NO, 5% NO₂, and 2% HONO on a mole basis (note by convention, total NO_x mass emissions are stated assuming all NO_x is emitted as NO₂). A summary of the emission inventory is provided below in Table 2. This emission inventory provides the basis for the modeling conducted in this study, and will be referred to as the 3× hot exhaust inventory (note however, that NO_x emissions were not increased above baseline EMFAC 7E values).

The August 27–29, 1987 SCAQS experiment covered a period running from Thursday through Saturday. Unfortunately, no weekend traffic activity data were available, so the motor vehicle emission inventory for August 29 was created using typical weekday traffic patterns which were not appropriate for a Saturday. Because of this problem, it was decided to focus on August 28 (Friday) when assessing airshed model performance.

The main objective of this study was to examine the effects of chemical composition of direct NO_x emissions on air pollutant concentrations. For this purpose, a 4 by 3 matrix of airshed model calculations was performed using

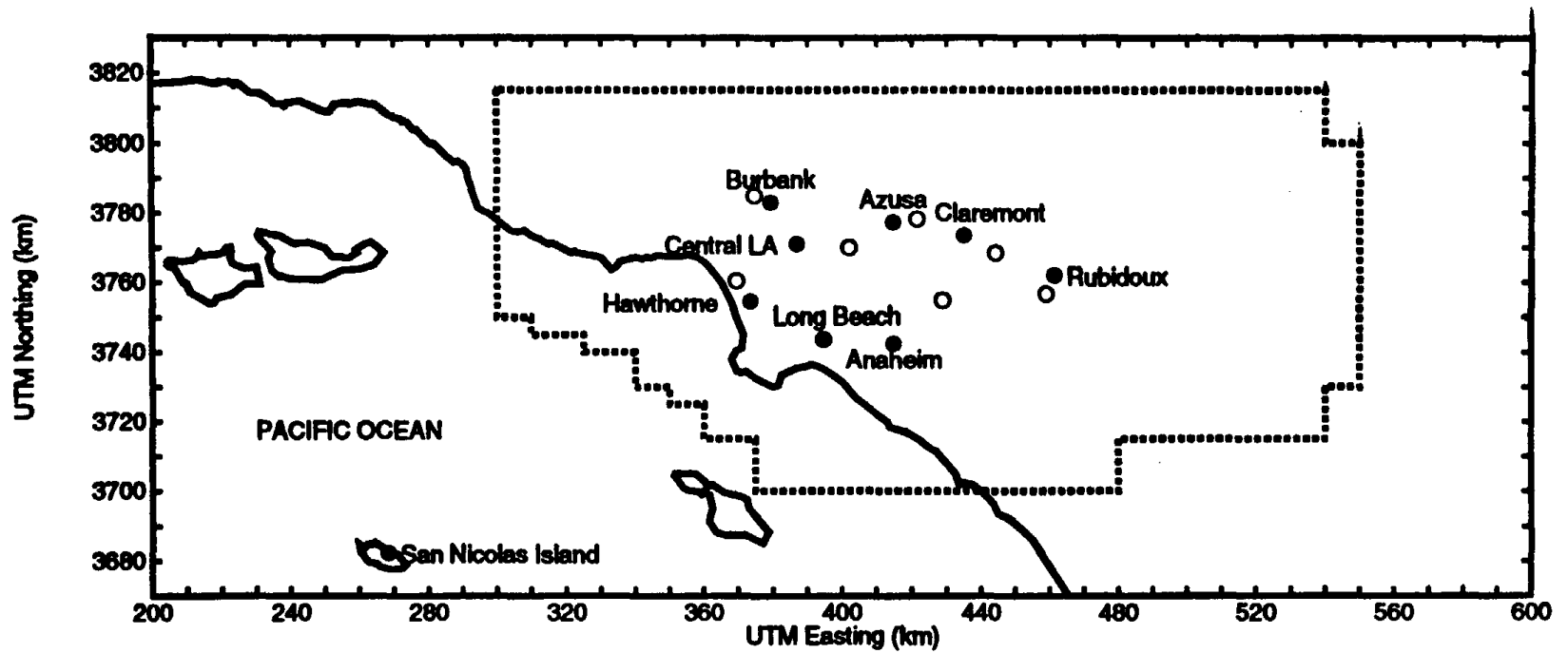


Figure 2. Map showing Southern California Air Quality Study air monitoring sites (solid circles) and upper air sounding sites (open circles). Note that both air quality measurements and upper air soundings were performed at Long Beach. The airshed model computational region boundary is indicated by the dashed line.

Table 2: Summary of SoCAB emission inventory for August 1987

species code	species description	emissions (10 ³ kg/day)
ALKA	C ₄ + alkanes	884
ETHE	ethene	114
ALKE	C ₃ + alkenes	190
TOLU	monoalkyl benzenes	178
AROM	di- and trialkyl benzenes	218
HCHO	formaldehyde	31
ALD2	acetaldehyde	24
MEK	ketones	51
MEOH	methanol	1
ETOH	ethanol & higher alcohols	235
ISOP	biogenic alkenes	117
ROG	total reactive organic gases	2042
NONR	non-reactive organic gases	1129
CO	carbon monoxide	10867
NO _x	oxides of nitrogen	1138

Notes: includes South Coast Air Basin plus Ventura County and portions of the Southeast Desert Air Basin. EMFAC 7E emission factors for CO and VOC were scaled up to 3 times the baseline values.

Table 3: Scaling factors used to adjust NO_x emission speciation

	0% NO ₂	5% NO ₂	10% NO ₂
0% HONO	1.07/0.00/0.0	1.02/1.02/0.0	0.97/2.04/0.0
1% HONO	1.06/0.00/0.5	1.01/1.01/0.5	0.96/2.02/0.5
2% HONO	1.05/0.00/1.0	1.00/1.00/1.0	0.95/2.00/1.0
3% HONO	1.04/0.00/1.5	0.99/0.99/1.5	0.94/1.98/1.5

Note: scaling factors A/B/C shown in this table were applied to NO, NO₂, and HONO emissions, respectively, for the NO_x speciation sensitivity runs.

different HONO and NO₂ emission fractions relative to total NO_x emissions. With total NO_x emissions held constant, NO₂ fractions were set to 0, 5, and 10% of total NO_x, and HONO fractions were set to 0, 1, 2, and 3% of total NO_x emissions. These levels span the likely ranges of direct NO₂ and HONO emissions. The emission inventories with alternate NO_x speciation assumptions were developed using the 3× hot exhaust inventory (Table 2) and the scaling factors for components of total NO_x emissions shown in Table 3. An additional airshed model calculation was conducted with NO_x emissions from all sources reduced to 50% of 3× hot exhaust (base) values, to study the importance of mass emissions versus NO_x speciation in determining air pollutant concentrations. In the reduced NO_x emissions case, the composition of NO_x used was again 93% NO, 5% NO₂, and 2% HONO.

Another objective of this study was to assess model performance in predicting concentrations of HONO, HNO₃, NH₃, and ammonium nitrate aerosol. Baseline model performance has already been assessed for ozone, NO₂, PAN, and lumped VOC (Harley et al., 1993ab). Available concentration data for nitrogen-containing air pollutants are reviewed below.

3.3 Observed Pollutant Concentrations

SCAQS Sampler

A special air sampling system to collect gaseous and size-resolved particulate matter samples was developed for SCAQS (Fitz et al., 1989) and deployed at the network of 9 ambient air monitoring sites shown in Figure 1. During the summer portion of SCAQS, 5 samples per day were collected at each site, from 0000–0500, 0500–0900, 0900–1300, 1300–1700, and 1700–2400 hours PST.

Line 3 of the SCAQS sampler measured fine particle nitrate quantitatively, using a fluorocarbon polymer-coated cyclone inlet to remove coarse particles, and a tubular denuder to remove nitric acid, upstream of a filter pack with a Teflon front filter and a nylon back filter. The nitric acid denuder consisted of ten 6 mm outer diameter tubes coated with magnesium oxide (Fitz et al., 1989). Line 4 of the SCAQS sampler was identical to line 3, except that it did not include the nitric acid denuder. Nitric acid concentrations were determined as the difference between total gas and particle nitrate (line 4) and particle nitrate alone (line 3). Teflon and nylon filters from lines 3 and 4 of the SCAQS sampler were extracted using 20 mL of 0.003 M NaHCO₃ / 0.0024 M Na₂CO₃ solution and quantified for nitrate by ion chromatography (Countess, 1989).

Ammonia concentrations were measured using oxalic acid-coated glass tubular denuders. Downstream of the ammonia denuder on line 5 of the SCAQS sampler, an oxalic acid-impregnated quartz filter was used to collect fine particle ammonium. Note that lines 3, 4, and 5 were all drawn from the same sample air stream, and were passed through the same Teflon-coated cyclone to remove coarse particles. While the same nitric acid denuders were used during multiple sample periods, new ammonia denuders were installed for every sampling period. The ammonia denuders and oxalic acid-impregnated filters were extracted with 10 mL of 0.0036 M sodium acetate solution; ammonium ion concentrations were then determined colorimetrically (Countess, 1989). In principle, this method yielded separate methods of gas-phase ammonia (line 5a) and fine particle ammonium (line 5b). However, the ammonia denuders were sometimes overloaded, mainly at the Rubidoux air monitoring site where ammonia concentrations were high-

est. Therefore, true ammonia concentrations at Rubidoux may at times be higher than the reported values.

Nitrous Acid

Spectroscopic (DOAS) measurements of ambient nitrous acid concentrations during SCAQS have been reported by Winer and coworkers (Winer, 1989; Winer and Biermann, 1994). During summer SCAQS sampling, HONO was detected overnight at the Claremont monitoring site, but was almost always below the detection limit of 0.8 ppb at Long Beach. Higher concentrations of HONO were measured at Long Beach during the fall portion of SCAQS.

Peroxyacetyl Nitrate

Williams and Grosjean (1990) measured PAN concentrations by electron capture gas chromatography at all of the SCAQS intensive monitoring sites shown in Figure 2, except for Hawthorne at the coast. The highest PAN concentrations were reported at Claremont.

Nitrogen Dioxide

Chemiluminescent NO_x analyzers operated routinely over a network of 35 air monitoring sites in the South Coast Air Basin and surrounding areas. NO₂ concentrations were estimated as the difference between total reactive nitrogen (NO_y) and nitric oxide (NO). Winer (1989) measured NO₂ directly at Long Beach and Claremont during SCAQS using DOAS.

4 Results

A total of 13 airshed model simulations were performed for the August 27–29 SCAQS intensive monitoring period. As described earlier, a 4 by 3 matrix of NO_x speciation sensitivity runs were conducted using 0, 5, and 10% NO₂ fractions, as well as 0, 1, 2, and 3% HONO fractions of total NO_x emissions. In addition, model sensitivity to total NO_x mass emissions was studied by reducing NO_x emissions by 50%. Time series plots showing airshed model predictions and observations for O₃ and the relevant nitrogenous air pollutants are included as Appendix A to this report, for all of the on-shore intensive monitoring sites shown in Figure 2.

Statistical measures of model performance for ozone and nitrogen-containing air pollutants are presented in Table 4. Statistical measures were calculated as described by Tesche et al. (1990). Model predictions and corresponding observations were only included in the performance statistics when observed concentrations were greater than or equal to cutoff levels shown in Table 4. Bias statistics indicate whether there is a systematic tendency of the model to overpredict or underpredict observed concentrations. Gross error statistics are computed using the absolute value of residuals (model prediction–observation). Therefore, overpredictions and underpredictions do not offset one another in the calculation of gross error. ARB guidelines (DaMassa, 1992) suggest that typical model performance *for ozone* is $\pm 15\%$ normalized bias and less than 35% normalized gross error.

Ozone

Performance statistics for ozone shown in Table 4 meet ARB guidelines for typical model performance. The normalized bias of +2% suggests that there was no systematic underprediction of ozone concentrations. However, peak ozone concentrations at inland sites such as Azusa and Claremont were underpredicted by the model, as shown in Figure A.1. Predicted ozone concentrations increased with increasing NO₂ and HONO fractions, as shown in Figures A.1 and A.2 respectively. However, the effects were small over the ranges of NO₂ and HONO fractions studied here. In Table 5, model predictions for ozone are presented for all of the possible combinations of HONO and NO₂ emission fractions listed in Table 3. Predicted ozone concentrations increased with increases in both HONO and NO₂ fractions. A difference of 9 ppb was found between the lowest and highest predicted ozone concentrations for the peak hour at Claremont. This increase in predicted ozone corresponds to an increase from 0 to 10% NO₂ fraction, and a simultaneous increase from 0 to 3% HONO in direct NO_x emissions.

Reductions of total NO_x mass emissions had a much larger effect on predicted ozone concentrations, as shown in Figure A.3. Predicted ozone concentrations from central Los Angeles east to Azusa increased significantly when NO_x emissions were reduced. In contrast, predicted ozone concentrations decreased at Rubidoux and increased only slightly at Claremont in response to reduced NO_x emissions. The spatial pattern of predicted ozone concentrations and the response to a 50% reduction in NO_x emissions are shown in Figures B.1 and B.2 respectively.

Nitrogen Dioxide

Predicted $\text{NO}_y\text{-NO}$ (i.e., total of NO_2 plus other reactive nitrogen species minus NO) concentrations were sensitive to the level of NO_2 emissions overnight, but did not show any response during the daytime (see Figure A.4). As expected, increased NO_2 emissions led to higher predicted NO_2 concentrations. The spatial distribution of true NO_2 concentrations is shown in Figure B.3. The highest predicted NO_2 concentrations in the afternoon occur in the eastern portion of Los Angeles county. Predicted NO_2 concentrations decrease significantly when NO_x emissions are reduced, as shown in Figure B.4. Changes in predicted total NO_2 concentrations at the central Los Angeles monitoring site are shown in Table 5 for all of the NO_x emission speciation cases.

Nitrous Acid

Predicted HONO concentrations were very sensitive to HONO emissions, as shown in Figure A.5. During the August 27–29 period, HONO concentrations were measured only at the Claremont and Long Beach monitoring sites. Predicted concentrations show the same diurnal pattern as that observed at Claremont: a build-up of HONO overnight and negligible daytime concentrations. Observed HONO concentrations at Claremont were predicted accurately on August 28, but were underpredicted on the morning of Saturday, August 29. Observed HONO concentrations at Long Beach were consistently low (usually below the detection limit of 0.8 ppb), and were overpredicted by the model. Predicted HONO concentrations as a function of NO_x emission speciation are also presented in Table 5.

Nitric Acid

Peak observed nitric acid concentrations were observed during the middle of the day, as shown in Figure A.6. Predicted concentrations exhibited a similar strong diurnal variation in nitric acid concentrations. Note that the observations shown in Figure A.6 were calculated by the denuder difference method from SCAQS sampler data, which means that observations are average values integrated over periods of 4 h or more. The highest nitric acid concentrations were predicted at the Azusa and Claremont monitoring sites, with lower predicted and observed values to the east at Rubidoux and upwind at coastal and mid-basin sites. Predicted nitric acid concentrations were not sensitive to NO₂ or HONO emissions. As shown in Figure A.6, decreasing total NO_x emissions resulted in approximately proportional decreases in peak predicted nitric acid concentrations. Statistical measures of model performance for nitric acid presented in Table 4 indicate that nitric acid concentrations are overpredicted by the model. Inspection of Figure B.5 indicates that high nitric acid concentrations occur in the downwind portions of the air basin. High ammonia emissions in the southwest corner of San Bernardino county were predicted to cause significant conversion of nitric acid to fine particle ammonium nitrate, as shown clearly in Figures B.5 and B.7. Reductions in NO_x emissions led to lower ambient nitric acid concentrations throughout the air basin, as shown in Figure B.6.

Fine Particle Nitrate

Observed fine particle ($D_p < 2.5 \mu\text{m}$) nitrate concentrations showed similar diurnal variation to that observed for nitric acid. The highest predicted and observed concentrations of nitrate aerosol were seen at the Rubidoux mon-

itoring site. Predicted fine particle nitrate concentrations were sensitive to total NO_x mass emissions, but not to NO_2 or HONO emission fractions. In general, the reduction in fine particle nitrate concentrations shown in Figure A.7 was not proportional to the reduction in NO_x emissions, although reducing NO_x always led to some decrease in fine particle nitrate concentrations. The highest fine particle nitrate concentrations were predicted downwind of ammonia source-rich agricultural areas in San Bernardino county. Reductions in NO_x emissions led to significant reductions in predicted fine particle nitrate, as seen by comparing Figures B.7 and B.8.

Ammonia

Observed and predicted ammonia concentrations were low in most parts of the basin, as shown in Figure A.8. Much higher concentrations were predicted and observed at the Rubidoux monitoring site. High concentrations of ammonia also were observed at Burbank. Nighttime ammonia concentrations were overpredicted at Long Beach. When NO_x emissions were reduced by 50%, predicted ammonia concentrations increased.

Peroxyacetyl Nitrate

Predicted PAN concentrations follow the same diurnal pattern seen in the observations: concentrations are highest during the early afternoon hours. Absolute PAN concentrations are predicted accurately at all sites, except at Claremont where PAN was underpredicted, and at Anaheim where observed values were close to zero at all times. Predicted PAN concentrations increased when NO_x emissions were reduced.

Table 4: Summary of model performance statistics

Statistical measure	O ₃	total NO ₂	PAN	HNO ₃	particle nitrate
number of sites	50	35	7	8	8
cutoff ^a	60 ppb	20 ppb	4 ppb	2 ppb	1 $\mu\text{g m}^{-3}$
bias ^b	-2.8	+4.8	-1.6	+1.8	+4.7
normalized bias	+2%	+24%	-5%	+57%	+36%
gross error ^b	28	19	2.6	5.1	12
normalized gross error	27%	46%	26%	87%	77%
σ of residuals ^b	36	25	4.2	6.4	17

Notes: ^aStatistical measures are calculated using all pairs of predicted and observed concentrations where the observed value is greater than or equal to the cutoff value shown above. ^bSame units as shown for the cutoff concentration. HNO₃ and fine particle nitrate observations are from the SCAQS sampler, integrated over periods of 4 h or more. Model predictions for these species were averaged over the same intervals; each sampling period was counted as a single observation.

Table 5: Effects of NO_x Emission Speciation on Airshed Model Predictions

O₃ (ppb) at Claremont, 1400-1500 hours PST

	0% NO ₂	5% NO ₂	10% NO ₂
0% HONO	175	177	178
1% HONO	177	178	180
2% HONO	178	180	182
3% HONO	180	182	184

HONO (ppb) at Central LA, 0500-0600 hours PST

	0% NO ₂	5% NO ₂	10% NO ₂
0% HONO	1.5	1.5	1.6
1% HONO	2.7	2.7	2.7
2% HONO	3.6	3.7	3.7
3% HONO	4.7	4.7	4.7

NO₂^{*} (ppb) at Central LA, 0500-0600 hours PST

	0% NO ₂	5% NO ₂	10% NO ₂
0% HONO	49	59	67
1% HONO	50	59	68
2% HONO	51	60	69
3% HONO	52	61	70

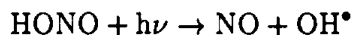
Note: all model predictions are for Aug. 28, 1987. NO₂^{*} concentrations include NO₂ and other species such as PAN and HONO that are measured as if they were NO₂ by chemiluminescent analyzers (see text for further discussion).

5 Discussion

Model predictions of the impact of NO_x emission speciation are directionally consistent with theoretical considerations. The photostationary state relationship (Seinfeld, 1988) predicts:

$$[\text{O}_3]_{ss} \propto \frac{[\text{NO}_2]}{[\text{NO}]}$$

and therefore increasing the NO_2 fraction of direct NO_x would lead to increased ambient O_3 concentrations. However, the magnitude of this influence appears to be small over the range of NO_2 fractions (0-10% of total NO_x) studied here. Ambient NO_2 concentrations during the daytime are determined by the rates of NO_2 photolysis and in situ NO to NO_2 conversion, but not by direct NO_2 emissions. The influence of NO_2 emissions is greater at night when sunlight-driven reactions do not occur. Likewise, increased emissions of HONO accelerate the initiation phase of the photochemical smog system by supplying additional hydroxyl radicals shortly after sunrise:



While Winer and Biermann (1994) found that nitrous acid photolysis was the dominant early morning initiation step at Long Beach on Nov. 12, 1987, HONO concentrations observed during the summer phase of SCAQS were not as high as those observed on Nov. 12, and HONO photolysis was therefore less important. Model results presented here indicate that even in the absence of any direct HONO emissions, other reactions such as formaldehyde photolysis

are capable of rapidly initiating photochemical reactions. NO_x emission speciation has a much greater influence on ambient HONO concentrations than it does on ozone concentrations. Further study of surface/heterogeneous formation pathways will be needed to understand the dynamics of atmospheric HONO concentrations completely.

Ozone concentrations were not sensitive to the distribution of NO_x emissions among NO, NO_2 , and HONO. In contrast, predicted ozone concentrations increased significantly in response to reductions in total NO_x mass emissions. The largest increases were seen in the source-rich western portion of the air basin. These results must be interpreted with caution however, because California is pursuing a control strategy that involves reductions in both VOC and NO_x emissions, not NO_x emissions alone as considered here. The analysis presented here was only intended to compare the importance of NO_x mass emissions and NO_x speciation. In general, NO_x mass emission rates were found to be more important than NO_x speciation in determining ambient pollutant concentrations.

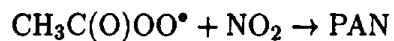
Nitric acid concentrations were overpredicted on average, as shown in Figure A.6. The overpredictions were large at Azusa and Rubidoux, whereas nitric acid concentrations were more accurately predicted at other sites such as Burbank, central Los Angeles, and Claremont. If ammonia emissions were higher, more nitric acid would be converted to ammonium nitrate by the time polluted air masses reached Rubidoux. Uncertainties in NO_x emissions, the dry deposition rate of nitric acid, and the equilibrium assumption for ammonium nitrate may have contributed to the overprediction of nitric acid concentrations.

Ammonia concentrations increased when NO_x emissions were reduced.

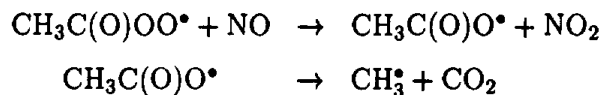
This occurred because nitric acid concentrations decreased in response to NO_x emission reductions, so that less ammonium nitrate could be formed, and more ammonia therefore remained in the gas phase. While observed ammonia concentrations at most sites were low during the August 27–29 episode, high concentrations were measured overnight at Burbank and during the morning at Rubidoux. Observed ammonia concentrations at Rubidoux (see Figure A.8) suggest that ammonia emissions may be more broadly distributed over the entire day, as compared to the present emission inventory which peaks sharply at midday. Some new information (Schmidt and Winegar, 1996) on ammonia emissions from dairy farms has been reported since the 1987 SCAQS ammonia emission inventory was compiled. However, further development of the ammonia emission inventory is needed, to include: accurate diurnal variation in emissions, up-to-date livestock populations in the South Coast Air Basin, and new measurements of ammonia emissions from cattle and poultry farms.

The large increase observed in aerosol nitrate concentrations between Claremont and Rubidoux suggests that control of ammonia and NO_x emissions could have significant air quality benefits in one of the basin's most polluted areas. However, emission forecasts for California through the year 2010 indicate that NO_x emissions will not be controlled nearly as effectively as emissions of CO and VOC (ARB, 1993). In the near term, since the prospect for large reductions in NO_x emissions appears bleak, the state should study the control of ammonia emissions from agricultural sources, in order to reduce the contribution of aerosol nitrate to $\text{PM}_{2.5}$ concentrations in the eastern portion of the South Coast Air Basin. Further research is needed to assess the advantages and disadvantages of this control strategy.

Predicted PAN concentrations increased significantly when NO_x emissions were reduced. Since PAN is formed directly from NO₂, this result was not expected. However, lowering NO_x emissions clearly resulted in higher concentrations of ozone and radical species. The peroxyacetyl radical reacts with NO₂ to form PAN:



Reaction with NO represents a competing sink for peroxyacetyl radicals:



As NO_x emissions (and therefore ambient NO_x concentrations) were reduced, peroxyacetyl and other radical concentrations increased. Since a greater fraction of the remaining NO_x was found in the form of NO₂, PAN formation was enhanced.

6 Conclusions

The impact of NO_x emissions and NO_x speciation on air pollutant concentrations was studied using the CIT airshed model applied to the August 27–29, 1987 SCAQS intensive monitoring period. A matrix of 12 airshed model calculations was conducted using a range of NO_2/NO_x and HONO/NO_x ratios in direct NO_x emissions. Daytime ambient NO_2 concentrations were determined by the rate of NO to NO_2 conversion in the atmosphere, not by direct NO_2 emissions. Predicted HONO concentrations were very sensitive to the HONO/NO_x emission ratio. Ozone and nitrogen-containing air pollutants other than NO_2 and HONO were not sensitive to NO_x emission speciation for the ratios examined in this study (0–10% NO_2 and 0–3% HONO). A 50% reduction in total NO_x mass emissions caused large changes in the concentrations of ozone and all nitrogen-containing air pollutants. NO_2 , HNO_3 , and particle nitrate concentrations decreased in response to reduced NO_x emissions, whereas PAN concentrations increased.

This is one of the first studies to examine airshed model performance systematically for ozone and nitrogen-containing species including nitric acid and fine particle nitrate. Uncertainties in emissions of ammonia, NO_x , and VOC , must be reduced to support future modeling and control strategy development for nitrogen-containing air pollutants.

7 Recommendations

Priorities for further research are listed below from highest to lowest:

- Further improvements are needed to the ammonia emission inventory. Specific improvements include:
 - understanding of the diurnal variation in ammonia emissions
 - measurements of ammonia emissions from cattle and poultry farms
 - updated livestock population data for the South Coast Air Basin
- To understand the dynamics of HONO concentrations, improved characterization of heterogeneous processes converting NO_x to HONO in the atmosphere is needed.
- A potentially large source of direct NO_2 emissions is gas turbine power plants. Measurements of NO_2 as well as total NO_x emissions should be conducted to assess the magnitude of NO_2 emissions from these sources.

8 References

- ARB (1993). California emission trends, 1975–2010. Stationary Source Emission Inventory Branch, California Air Resources Board, Sacramento, CA.
- Berges, M. G. M., R. M. Hofmann, D. Scharffe and P. J. Crutzen (1993). Nitrous oxide emissions from motor vehicles in tunnels and their global extrapolation. *Journal of Geophysical Research* 98(D10), 18527-18531.
- Cadle, S. H., G. J. Nebel and R. L. Williams (1979). Measurements of unregulated emissions from General Motors light-duty vehicles. *SAE technical paper series*, no. 790694.
- Calvert, J. G., G. Yarwood and A. M. Dunker (1994). An evaluation of the mechanism of nitrous acid formation in the urban atmosphere. *Research on Chemical Intermediates* 20, 463-502.
- Countess, R. J. (1989). Southern California Air Quality Study SCAQS sampler chemistry. 82nd Annual Meeting of the Air & Waste Management Association, Anaheim, CA., paper no. 89-140.2.
- DaMassa, J. (1992). Technical guidance document: photochemical modeling. California Air Resources Board, Sacramento, CA.
- Dasch, J. M. (1992). Nitrous oxide emissions from vehicles. *Journal of the Air & Waste Management Association* 42, 63-67.
- Dickson, R. J. (1991). Development of the ammonia emission inventory for the Southern California Air Quality Study. Radian Corporation, Sacramento, CA.
- Finlayson-Pitts, B. J. and J. N. Pitts Jr. (1986). *Atmospheric chemistry: fundamentals and experimental techniques*. New York, Wiley.
- Fitz, D., M. Chan, G. R. Cass, D. R. Lawson and L. L. Ashbaugh (1989). A multi-component size-classifying aerosol and gas sampler for ambient air monitoring. 82nd Annual Meeting of the Air & Waste Management Association, Anaheim, CA, paper no. 89-140.1.

- Gery, M. W., G. Z. Whitten, J. P. Killus and M. C. Dodge (1989). A photochemical kinetics mechanism for urban and regional scale computer modeling. *Journal of Geophysical Research* 94(D10), 12925-12956.
- Gharib, S. and G. R. Cass (1984). Ammonia emissions in the South Coast Air Basin — 1982. Environmental Quality Laboratory, California Institute of Technology, Pasadena, CA.
- Harley, R. A., M. P. Hannigan and G. R. Cass (1992). Respeciation of organic gas emissions and the detection of excess unburned gasoline in the atmosphere. *Environmental Science & Technology* 26, 2395-2408.
- Harley, R. A., A. G. Russell, G. J. McRae, G. R. Cass and J. H. Seinfeld (1993a). Photochemical modeling of the Southern California Air Quality Study. *Environmental Science & Technology* 27, 378-388.
- Harley, R. A., A. G. Russell and G. R. Cass (1993b). Mathematical modeling of the concentrations of volatile organic compounds: model performance using a lumped chemical mechanism. *Environmental Science & Technology* 27, 1638-1649.
- Harris, G. W. (1987). Measurements of NO₂ and HNO₃ in diesel exhaust gas by tunable diode laser absorption spectroscopy. *Environmental Science & Technology* 21, 299-304.
- Harris, G. W., W. P. L. Carter, A. M. Winer, J. N. Pitts, U. Platt and D. Perner (1982). Observations of nitrous acid in the Los Angeles atmosphere and implications for predictions of ozone-precursor relationships. *Environmental Science & Technology* 16, 414-419.
- Harrison, R. M., and I. M. Msibi (1994). Validation of techniques for fast response measurement of HNO₃ and NH₃ and determination of the [NH₃][HNO₃] concentration product. *Atmospheric Environment* 28, 247-255.
- Heywood, J. B. (1988). *Internal combustion engine fundamentals*. New York, McGraw-Hill.
- Hilliard, J. C. and R. W. Wheeler (1979). Nitrogen dioxide in engine exhaust. *SAE technical paper series*, no. 790961.
- Hildemann, L. M., A. G. Russell and G. R. Cass (1984). Ammonia and nitric acid concentrations in equilibrium with atmospheric aerosols: experiment vs. theory. *Atmospheric Environment* 18, 1737-1750.
- Ingalls, M. N., L. R. Smith and R. E. Kirksey (1989). Measurement of on-road vehicle emission factors in the California South Coast air basin. Volume I: regulated emissions. Southwest Research Institute, San Antonio, TX.

Johnson, G. M. and M. Y. Smith (1978). Emissions of NO₂ from a large gas-turbine power station. *Combustion Science and Technology* 19, 67-70.

Kirchstetter, T. W., R. A. Harley and D. Littlejohn (1996). Measurement of nitrous acid in motor vehicle exhaust. Submitted to *Environmental Science & Technology*.

Lawson, D. R. (1990). The Southern California Air Quality Study. *Journal of the Air & Waste Management Association* 40, 156-165.

Lenner, M. (1987). Nitrogen dioxide in exhaust emissions from motor vehicles. *Atmospheric Environment* 21, 37-43.

Lenner, M., O. Lindqvist and A. Rosen (1983). The NO₂/NO_x ratio in emissions from gasoline-powered cars: high NO₂ percentage in idle engine measurements. *Atmospheric Environment* 17, 1395-1398.

Lurmann, F. W., W. P. L. Carter and L. A. Coyner (1987). A surrogate species chemical reaction mechanism for urban-scale air quality simulation models. ERT Inc., Newbury Park, CA and Statewide Air Pollution Research Center, Riverside, CA.

McRae, G. J., W. R. Goodin and J. H. Seinfeld (1982). Development of a second-generation mathematical model for urban air pollution-I. Model formulation. *Atmospheric Environment* 16, 679-696.

Muzio, L. J. and J. C. Kramlich (1988). An artifact in the measurement of N₂O from combustion sources. *Geophysical Research Letters* 15, 1369-1372.

Muzio, L. J., M. E. Teague, J. C. Kramlich, J. A. Cole, J. M. McCarthy and R. K. Lyon (1989). Errors in grab sample measurements of N₂O from combustion sources. *Journal of the Air Pollution Control Association* 39, 287-293.

Pierson, W. R., A. W. Gertler and R. L. Bradow (1990). Comparison of the SCAQS tunnel study with other on-road vehicle emission data. *Journal of the Air & Waste Management Association* 40, 1495-1504.

Pitts, J. N., H. W. Biermann, A. M. Winer and E. C. Tuazon (1984). Spectroscopic identification and measurement of gaseous nitrous acid in dilute auto exhaust. *Atmospheric Environment* 18, 847-854.

Pitts, J. N., T. J. Wallington, H. W. Biermann and A. M. Winer (1985). Identification and measurement of nitrous acid in an indoor environment. *Atmospheric Environment* 19, 763-767.

Pitts, J. N., T. J. Wallington, A. M. Winer and E. C. Tuazon (1989). Time-resolved identification and measurement of indoor air pollutants by spectroscopic techniques: gaseous nitrous acid, methanol, formaldehyde and formic acid. *Journal of the Air & Waste Management Association* 39, 1344-1347.

Russell, A. G., K. F. McCue and G. R. Cass (1988). Mathematical modeling of the formation of nitrogen-containing air pollutants. 1. Evaluation of an Eulerian photochemical model. *Environmental Science & Technology* 22, 263-271.

Russell, A. G., G. J. McRae and G. R. Cass (1983). Mathematical modeling of the formation and transport of ammonium nitrate aerosol. *Atmospheric Environment* 17, 949-964.

Sawyer, R. F. (1992). Reformulated gasoline for automobile emissions reduction. Twenty-fourth symposium (International) on combustion, The Combustion Institute, Pittsburgh, PA.

Schmidt, C.E., and E. Winegar (1996). Results of the measurement of PM₁₀ precursor compounds from dairy industry livestock waste: summer testing event. Report to the South Coast Air Quality Management District, Diamond Bar, CA.

Seinfeld, J. H. (1988). Ozone air quality models. A critical review. *Journal of the Air Pollution Control Association* 38, 616-645.

Sjödin, A. (1988). Studies of the diurnal variation of nitrous acid in urban air. *Environmental Science & Technology* 22, 1086-1089.

Sjödin, A., D. A. Cooper and K. Andreasson (1994). Estimations of real-world N₂O emissions from road vehicles by means of measurements in a traffic tunnel. *Journal of the Air & Waste Management Association* 45, 186-190.

Stelson, A. W. and J. H. Seinfeld (1982a). Relative humidity and temperature dependence of the ammonium nitrate dissociation constant. *Atmospheric Environment* 16, 983-992.

Stelson, A. W. and J. H. Seinfeld (1982b). Relative humidity and pH dependence of the vapor pressure of ammonium nitrate-nitric acid solutions at 25C. *Atmospheric Environment* 16, 993-1000.

Tesche, T. W., P. Georgopoulos, J. H. Seinfeld, G. R. Cass, F. W. Lurmann and P. M. Roth (1990). Improvement of procedures for evaluating photochemical models. Radian Corporation, Sacramento, CA. Final report to the California Air Resources Board under contract no. A832-103.

Vecera, Z. and P. K. Dasgupta (1991). Measurement of ambient nitrous acid and a reliable calibration source for gaseous nitrous acid. *Environmental Science & Technology* 25, 255-260.

Wagner, K. K. and P. D. Allen (1990). SCAQS emissions inventory for August 27-29, 1987 (tape ARA714). Technical Support Division, California Air Resources Board, Sacramento, CA.

Wexler, A. S., and J. H. Seinfeld (1990). The distribution of ammonium salts among a size and composition dispersed aerosol. *Atmospheric Environment* 24A, 1231-1246.

Wexler, A. S., F. W. Lurmann and J. H. Seinfeld (1994). Modeling urban and regional aerosols—I. Model development. *Atmospheric Environment* 28, 531-546.

Williams, E. L. and D. Grosjean (1990). SCAQS: peroxyacetyl nitrate. *Atmospheric Environment* 24A, 2369-2377.

Winer, A. M. (1989). Measurements of nitrous acid, nitrate radicals, formaldehyde, and nitrogen dioxide for the Southern California Air Quality Study by differential optical absorption spectroscopy. Statewide Air Pollution Research Center, University of California, Riverside, CA.

Winer, A. M. and H. W. Biermann (1994). Long pathlength differential optical absorption spectroscopy (DOAS) measurements of gaseous HONO, NO₂ and HCHO in the California South Coast Air Basin. *Res. Chem. Intermed.* 20, 423-445.

Winer, A. M., J. W. Peters, J. P. Smith and J. N. Pitts (1974). *Environmental Science & Technology* 8, 1118-1121.

A Time Series Plots

In this appendix, time series plots of predicted and observed pollutant concentrations are presented for the network of 8 mainland air monitoring sites shown previously in Figure 2. Each plot consists of two pages (4 sites per page), with the first page of each pair presenting model predictions and observations along a cross-section of the air basin from west to east starting at Hawthorne and proceeding inland through central LA to Claremont and Rubidoux. The figures are listed below:

- A.1 Ozone plots showing sensitivity to NO_2 emission fraction
- A.2 Ozone plots showing sensitivity to HONO emission fraction
- A.3 Ozone plots showing effects of NO_x emission reduction
- A.4 Total nitrogen dioxide (NO_y -NO) time series plots
- A.5 Nitrous acid time series plots
- A.6 Nitric acid time series plots
- A.7 Fine particle nitrate time series plots
- A.8 Ammonia time series plots
- A.9 Peroxyacetyl nitrate time series plots

Figure A.1: Ozone Time Series Plots -- NO2 Emission Impact
(HONO Emission Fraction Held Constant at 2%)

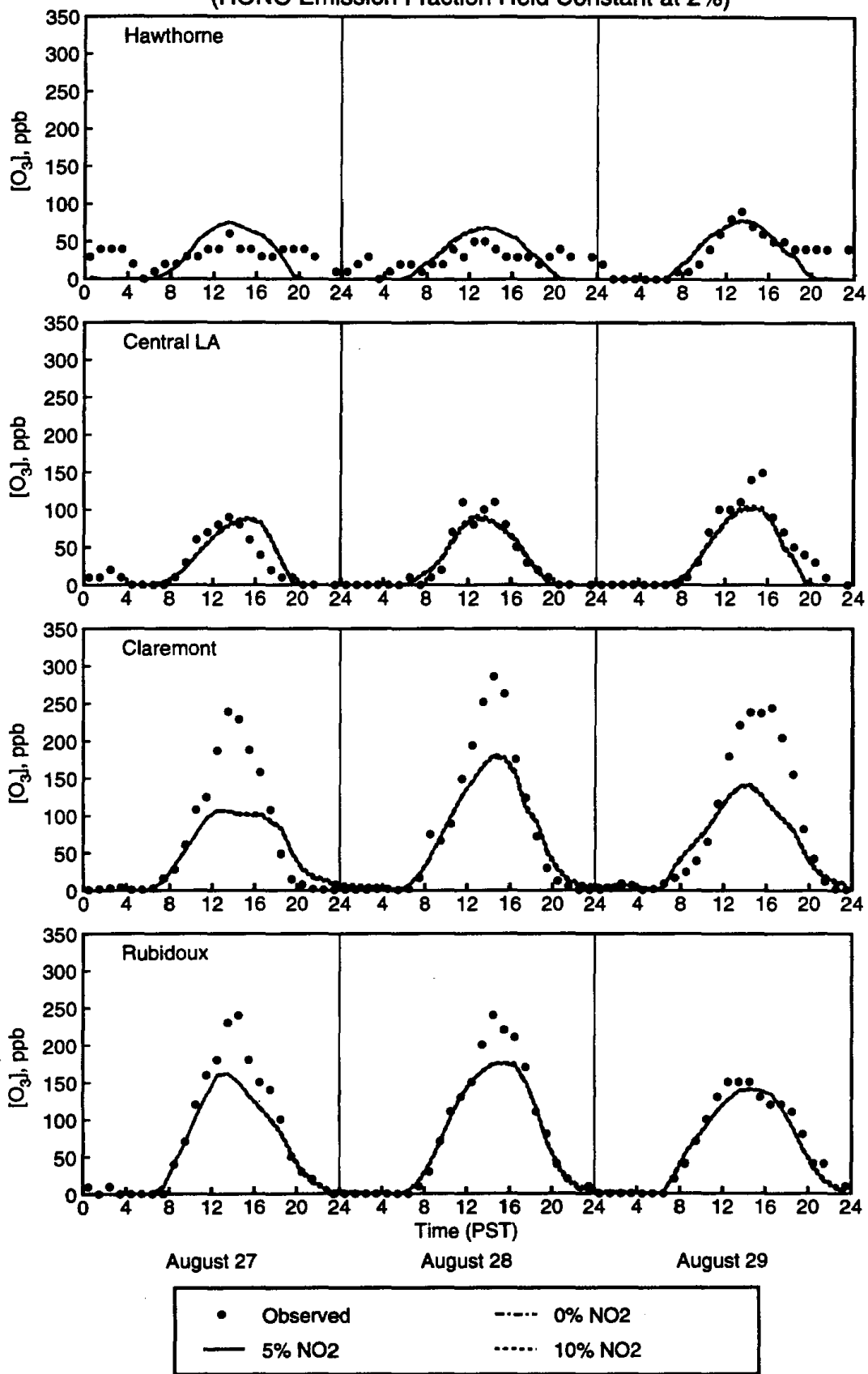


Figure A.1: Ozone Time Series Plots -- NO2 Emission Impact
(HONO Emission Fraction Held Constant at 2%)

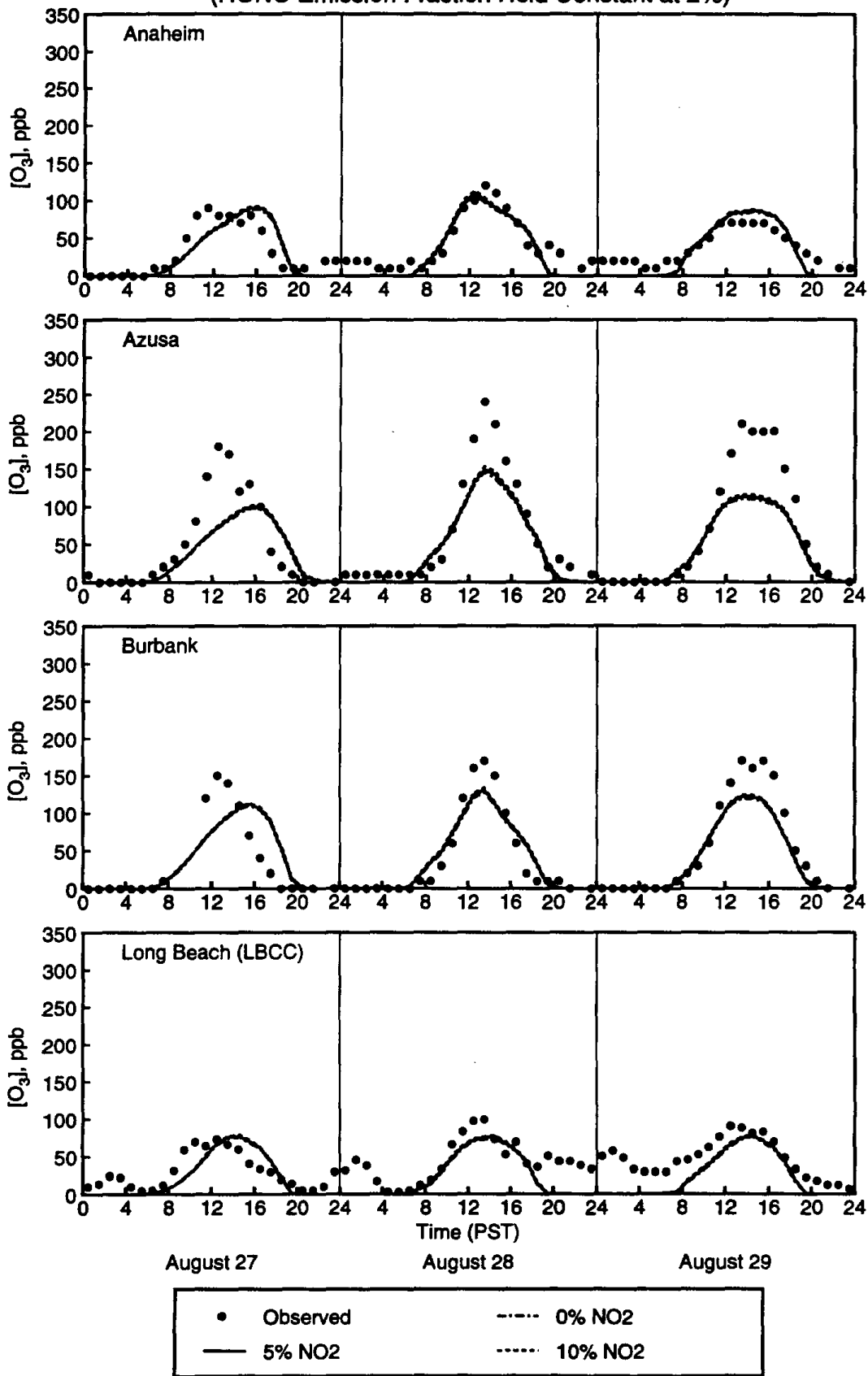


Figure A.2: Ozone Time Series Plots -- HONO Emission Impact
(NO₂ Emission Fraction Held Constant at 5%)

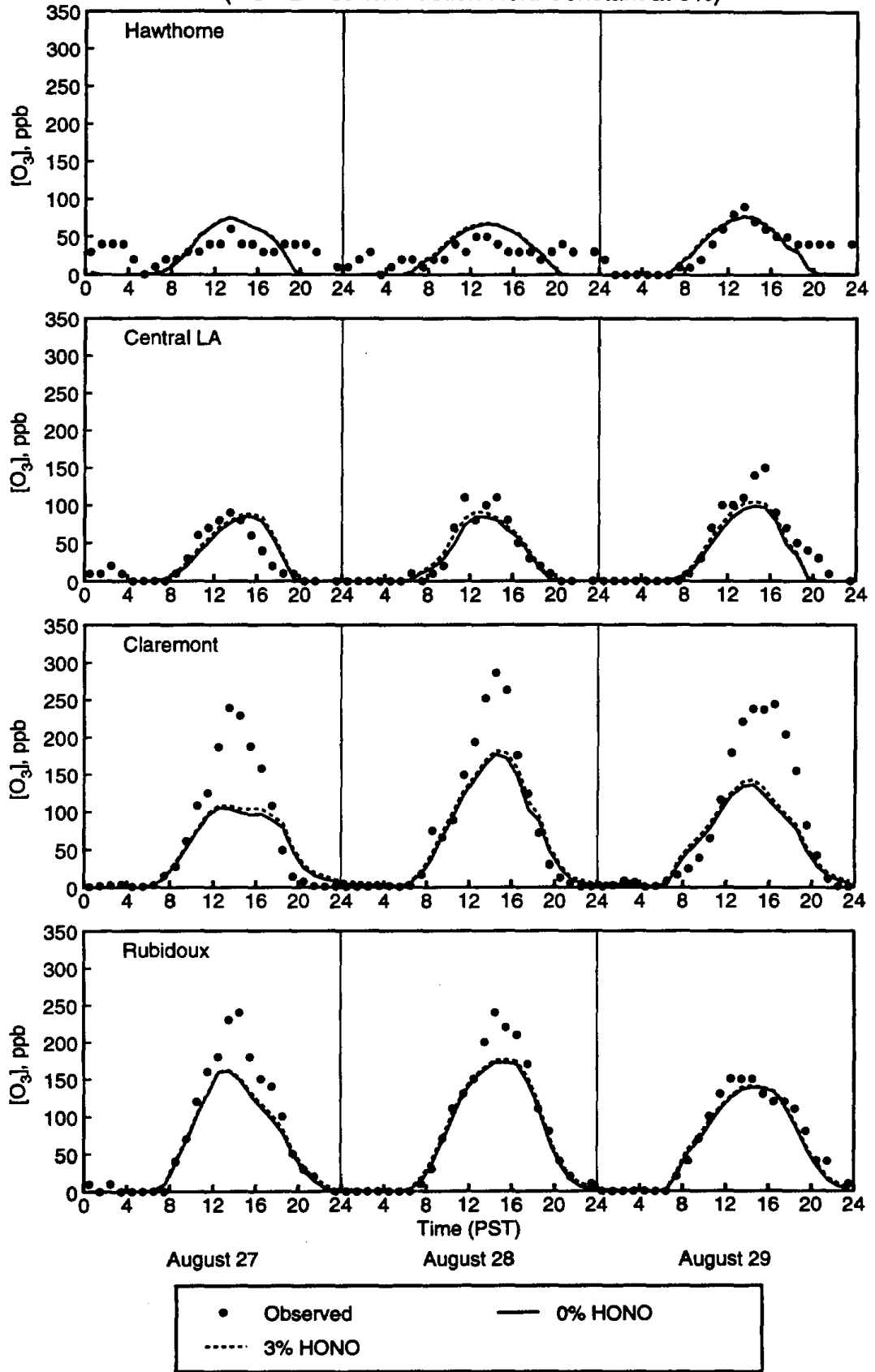


Figure A.2: Ozone Time Series Plots -- HONO Emission Impact
(NO₂ Emission Fraction Held Constant at 5%)

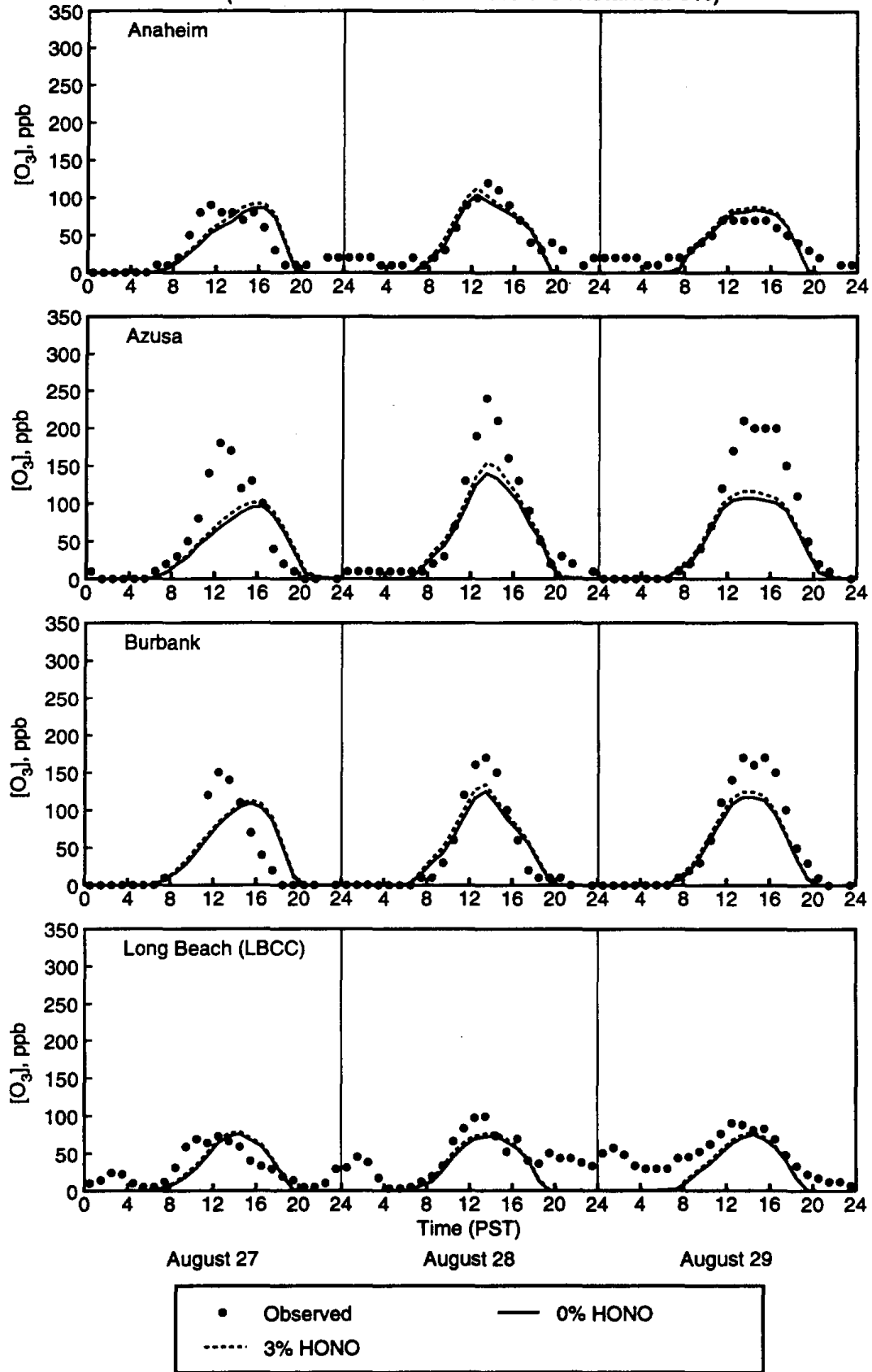


Figure A.3: Ozone Time Series Plots -- Impact of NOx Mass Emissions
(HONO Fraction=2% and NO2 Fraction=5%)

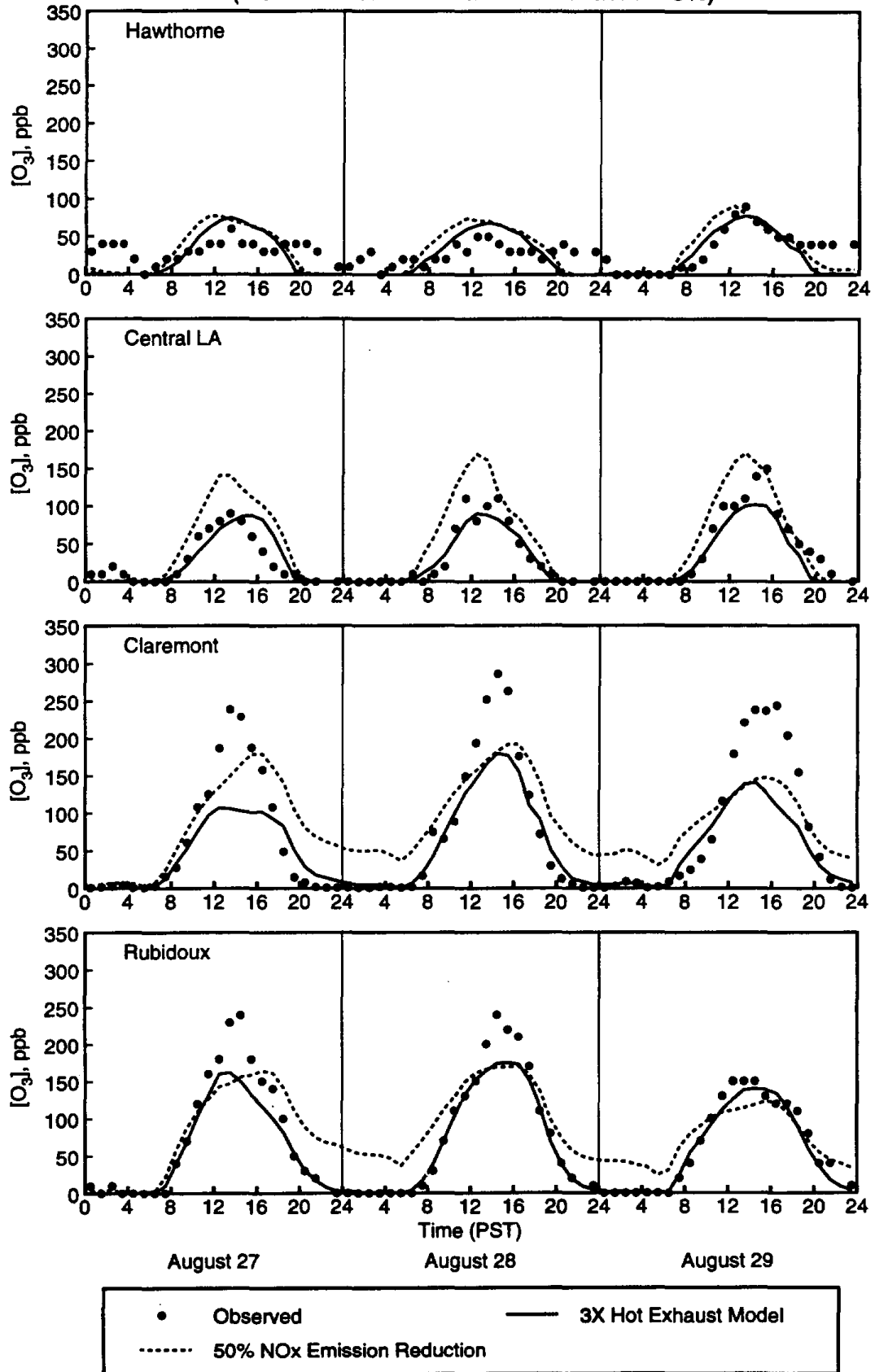


Figure A.3: Ozone Time Series Plots -- Impact of NOx Mass Emissions (HONO Fraction=2% and NO2 Fraction=5%)

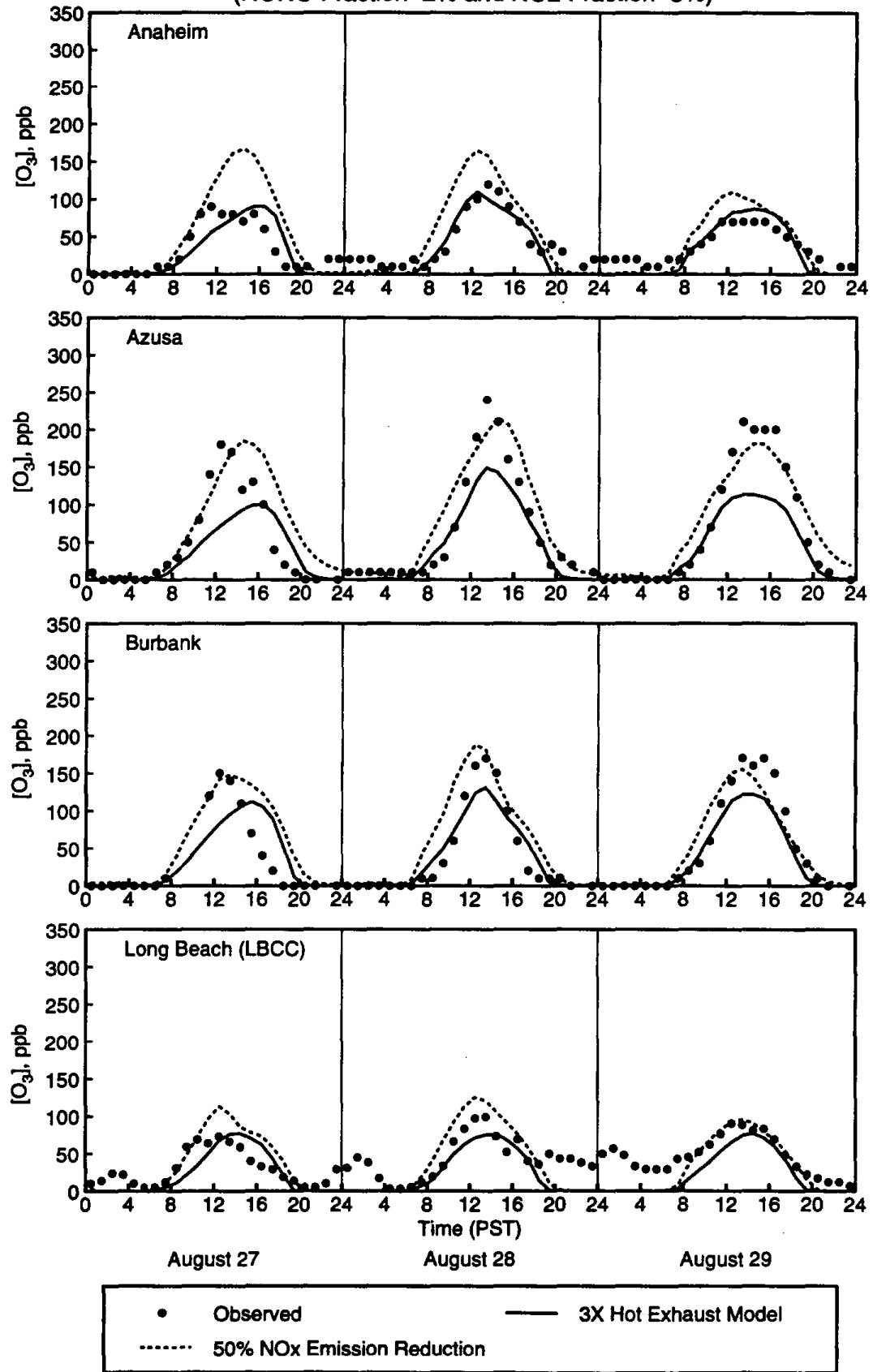


Figure A.4: Nitrogen Dioxide Time Series Plots
(HONO Emission Fraction Held Constant at 2%)

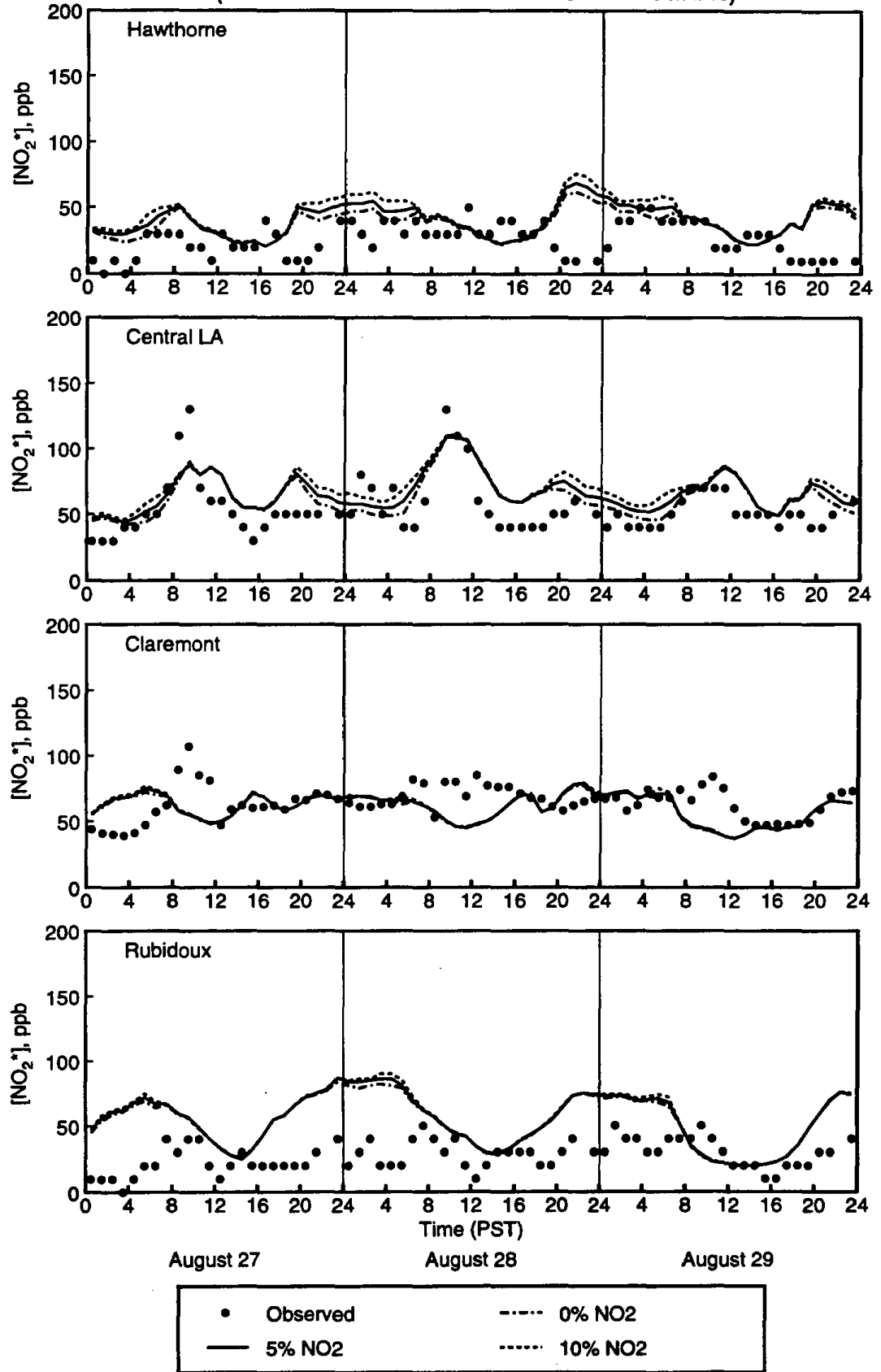


Figure A.4: Nitrogen Dioxide Time Series Plots
(HONO Emission Fraction Held Constant at 2%)

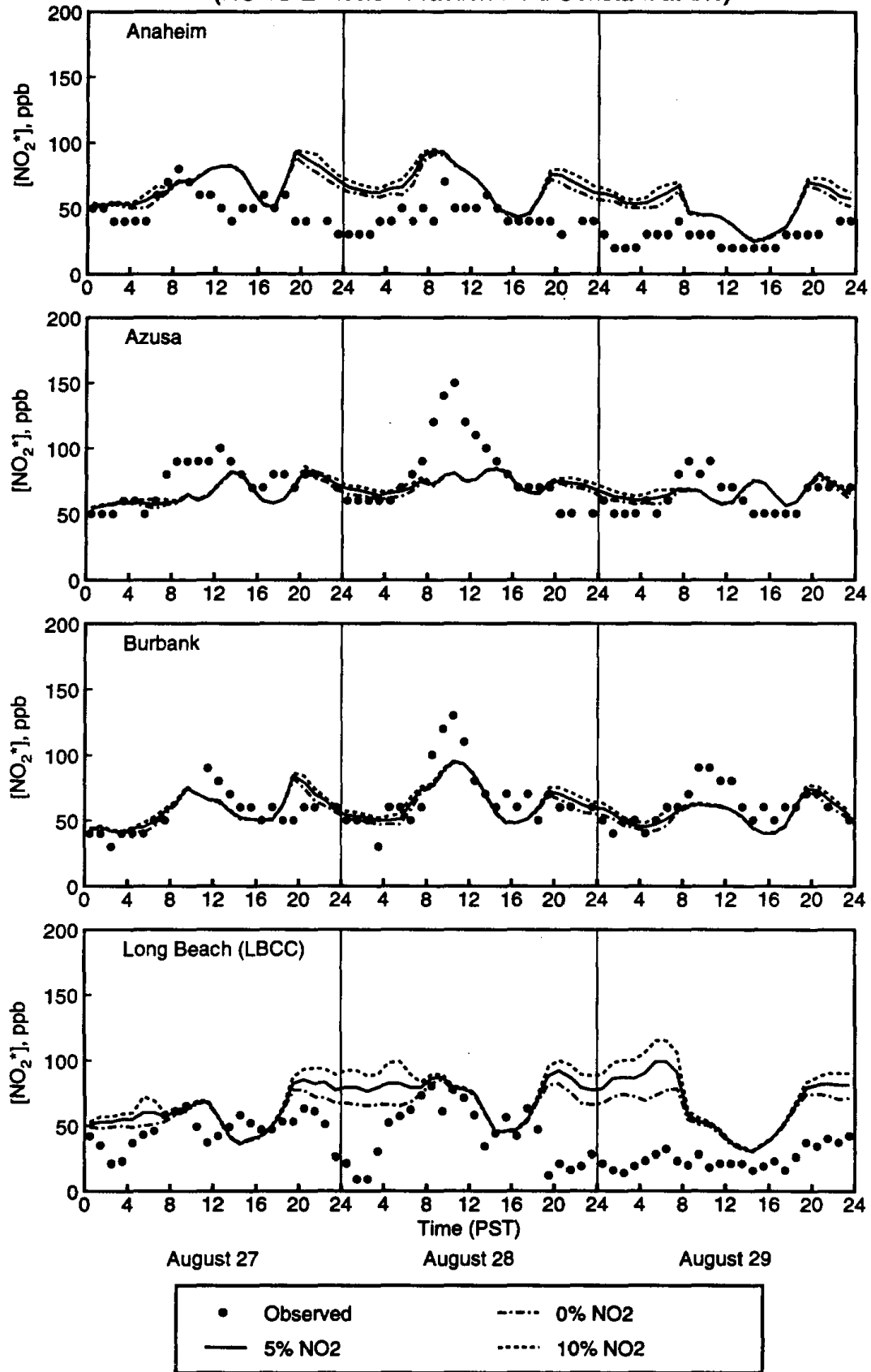


Figure A.5: Nitrous Acid Time Series Plots
(NO₂ Emission Fraction Held Constant at 5%)

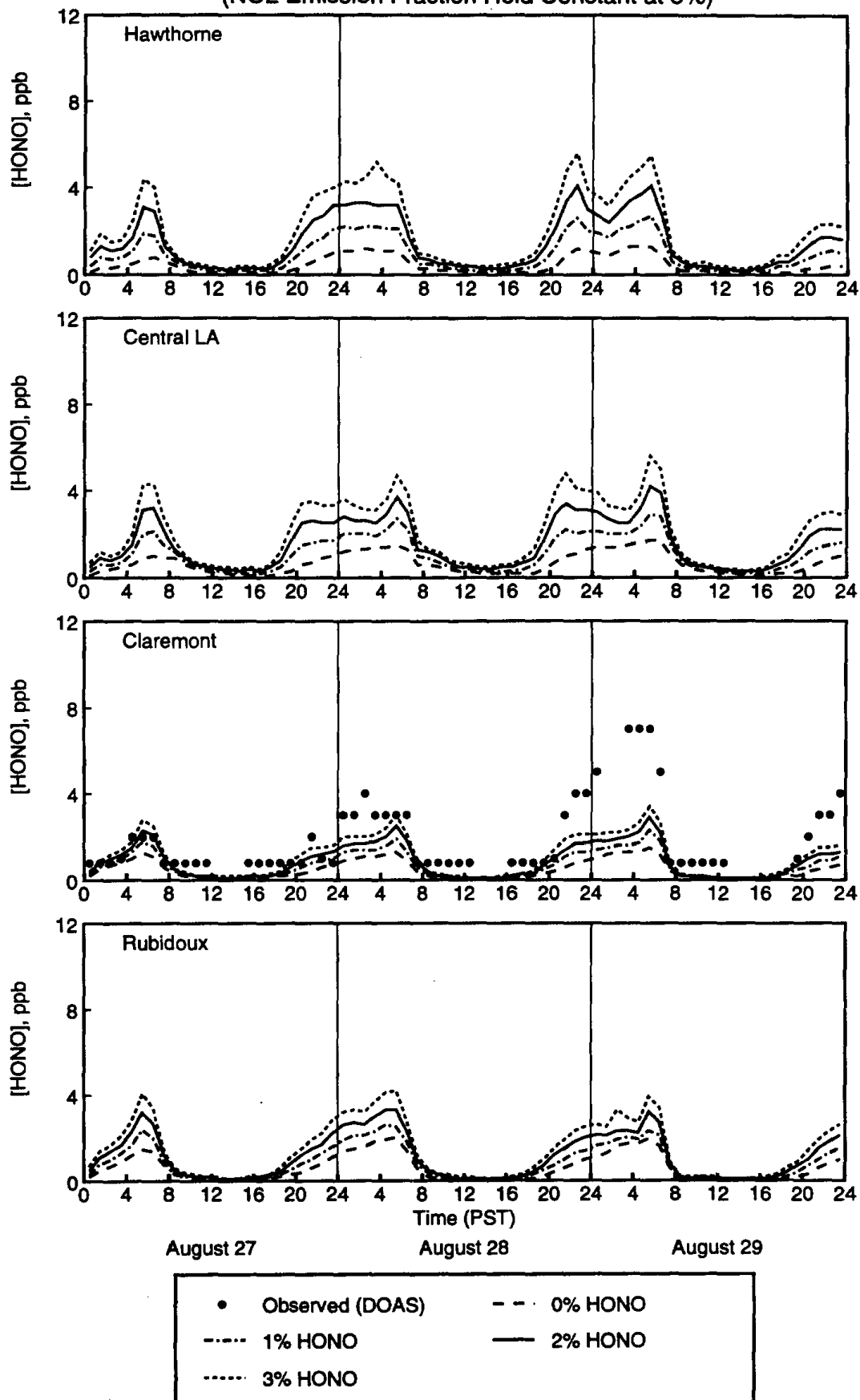


Figure A.5: Nitrous Acid Time Series Plots
(NO₂ Emission Fraction Held Constant at 5%)

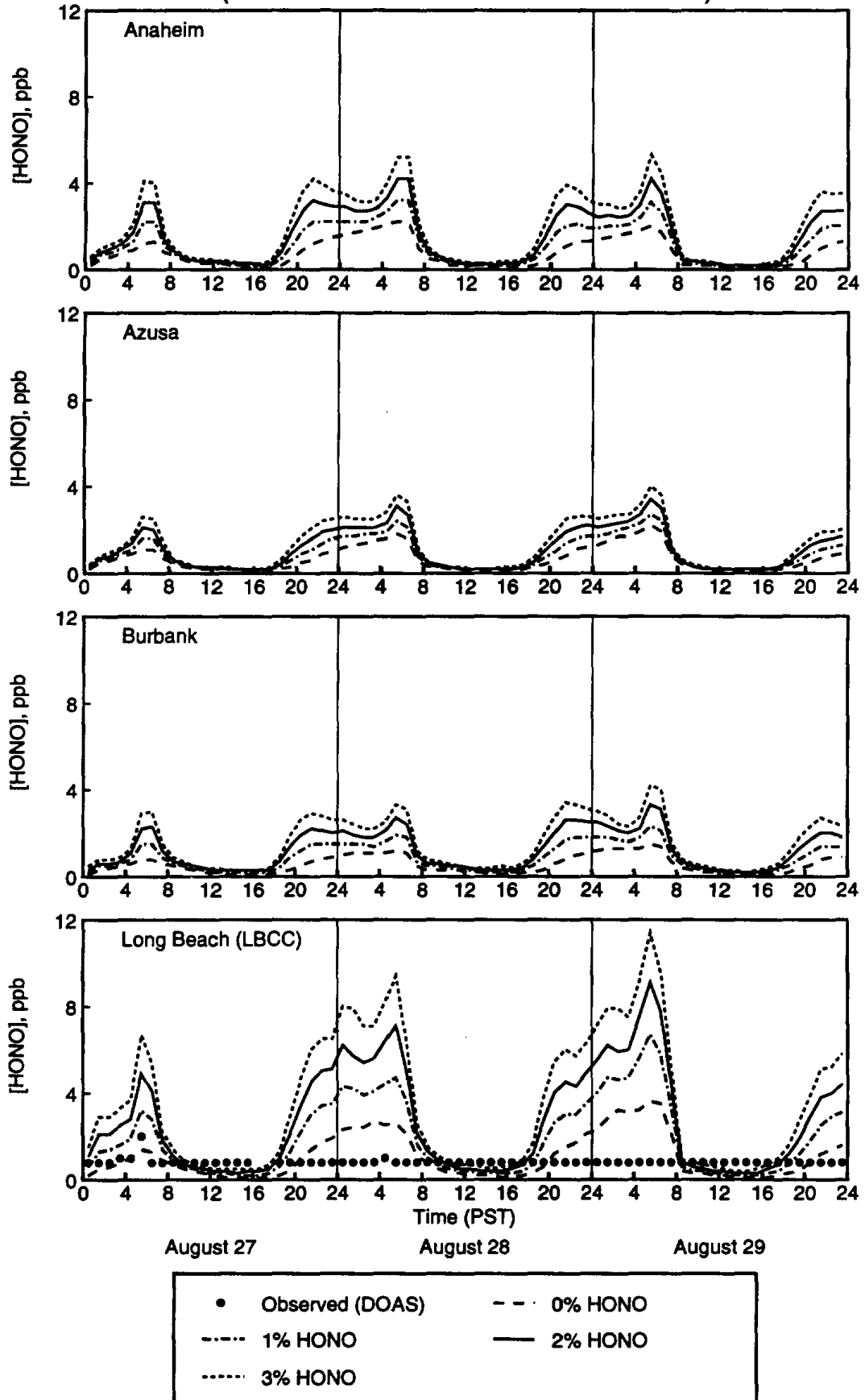


Figure A.6: Nitric Acid Time Series Plots
(HONO Fraction=2% and NO2 Fraction=5%)

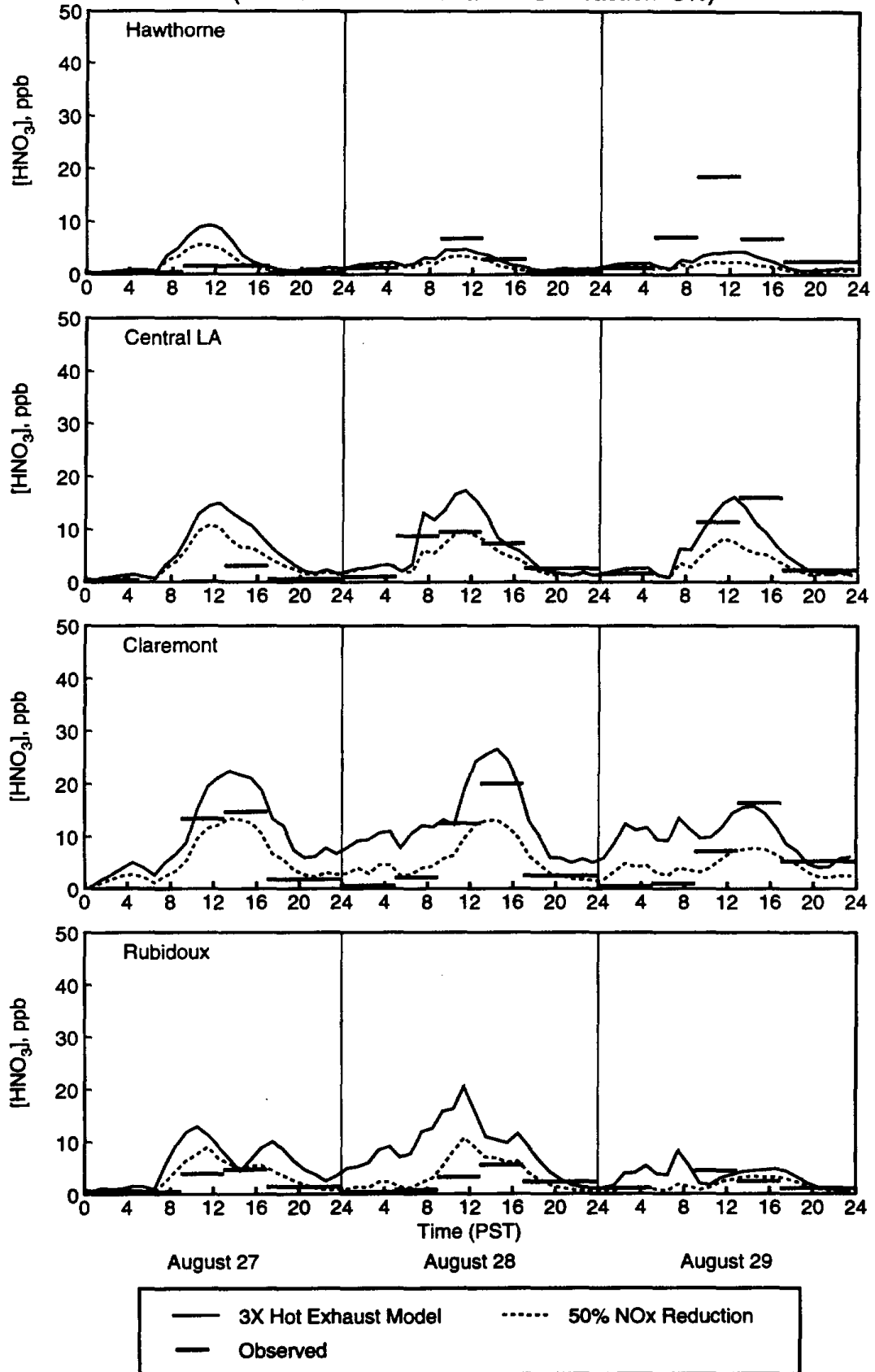


Figure A.6: Nitric Acid Time Series Plots
(HONO Fraction=2% and NO2 Fraction=5%)

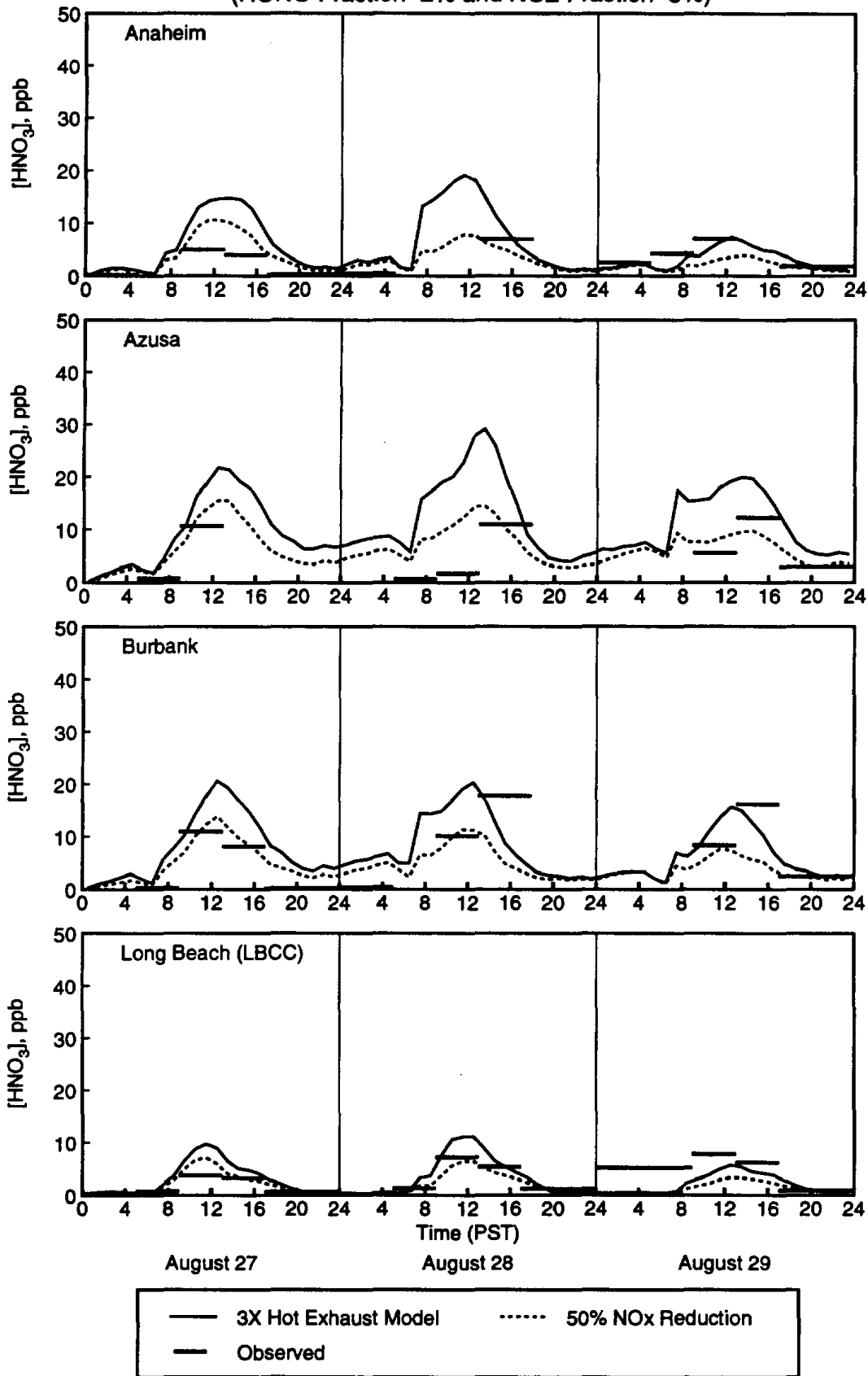


Figure A.7: Fine Particle Nitrate Time Series Plots
(HONO Fraction=2% and NO2 Fraction=5%)

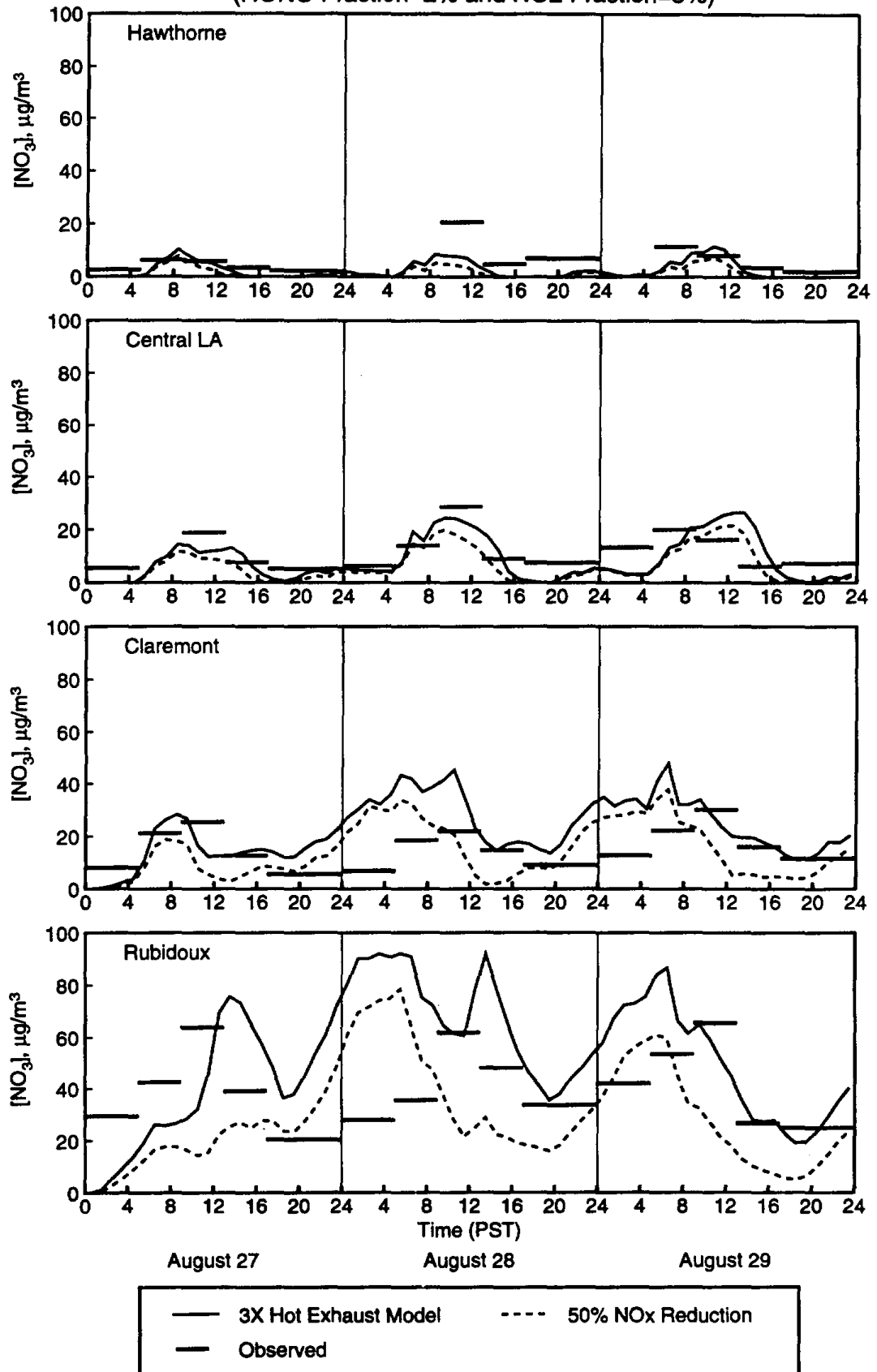


Figure A.7: Fine Particle Nitrate Time Series Plots
(HONO Fraction=2% and NO2 Fraction=5%)

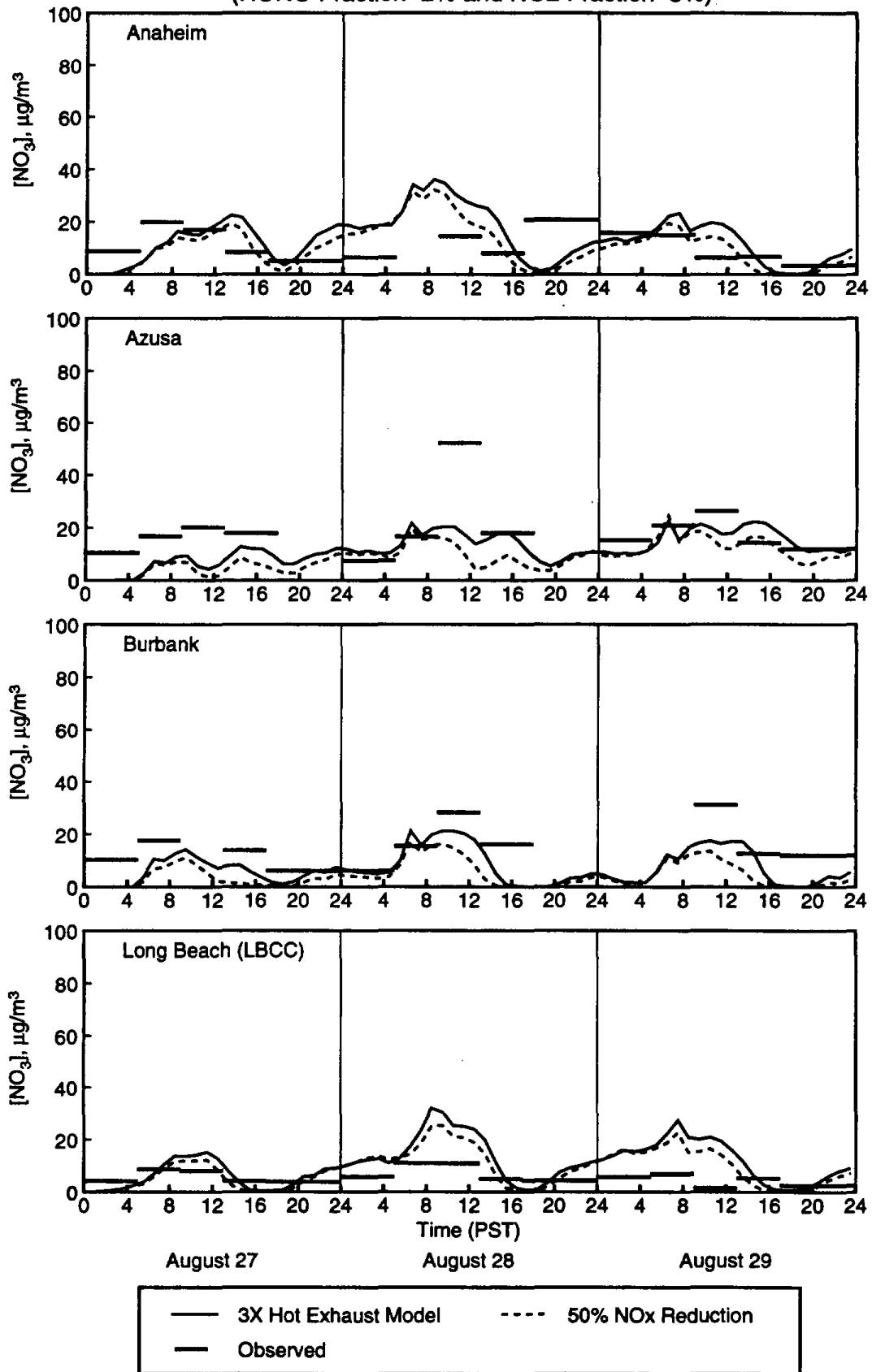


Figure A.8: Ammonia Time Series Plots
(HONO Fraction=2% and NO2 Fraction=5%)

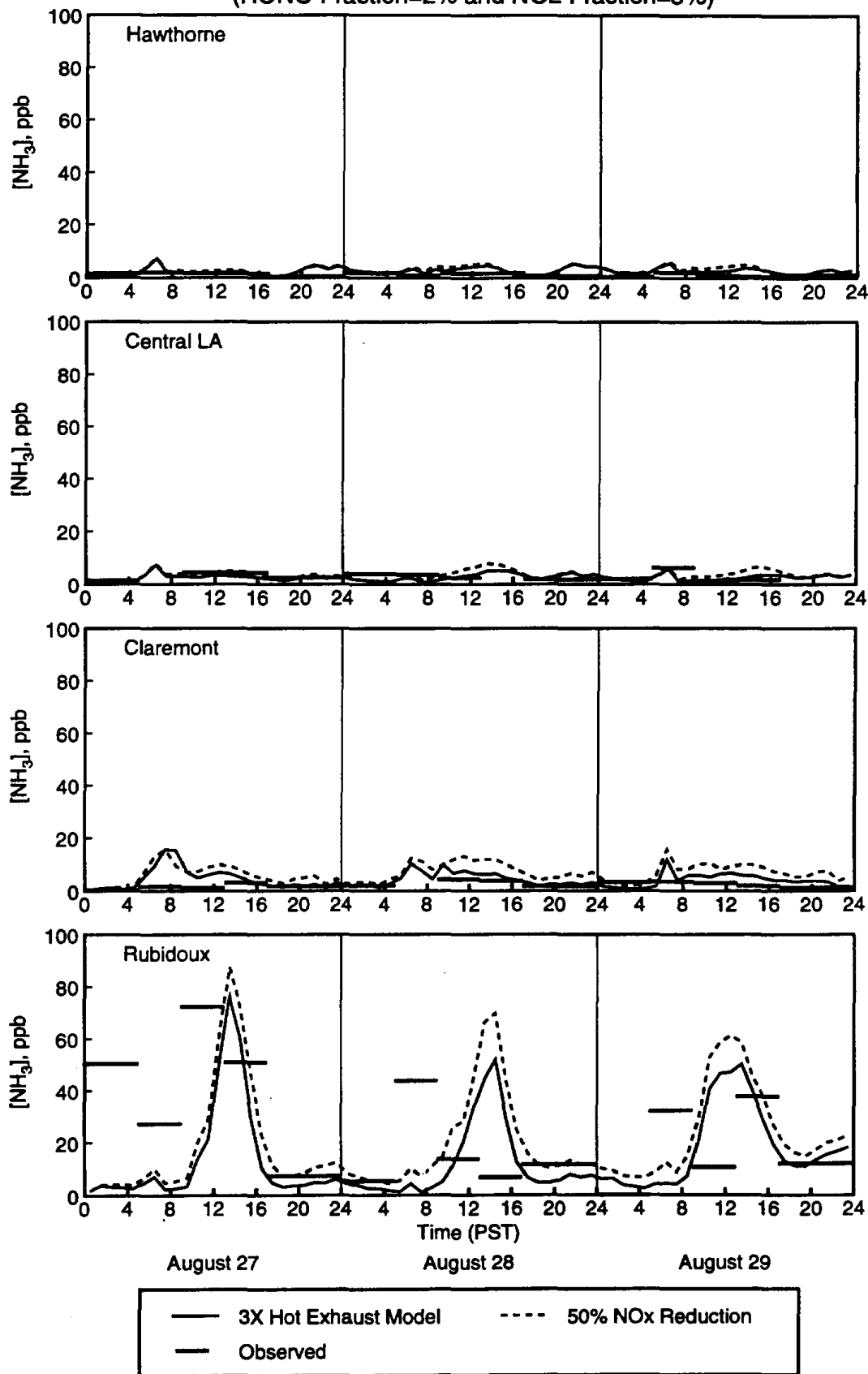


Figure A.8: Ammonia Time Series Plots
(HONO Fraction=2% and NO2 Fraction=5%)

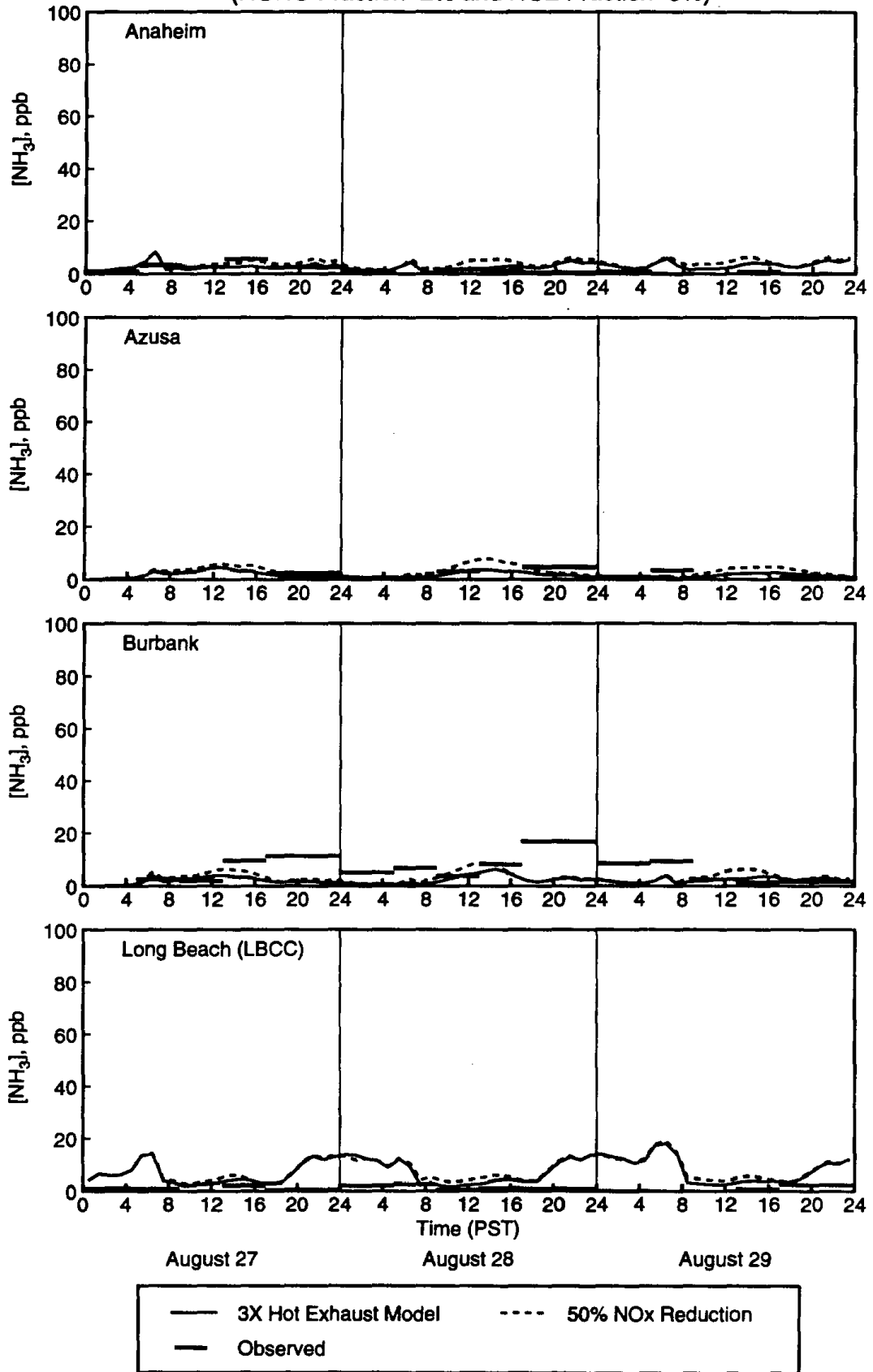


Figure A.9: Peroxyacetyl Nitrate Time Series Plots
(HONO Fraction=2% and NO2 Fraction=5%)

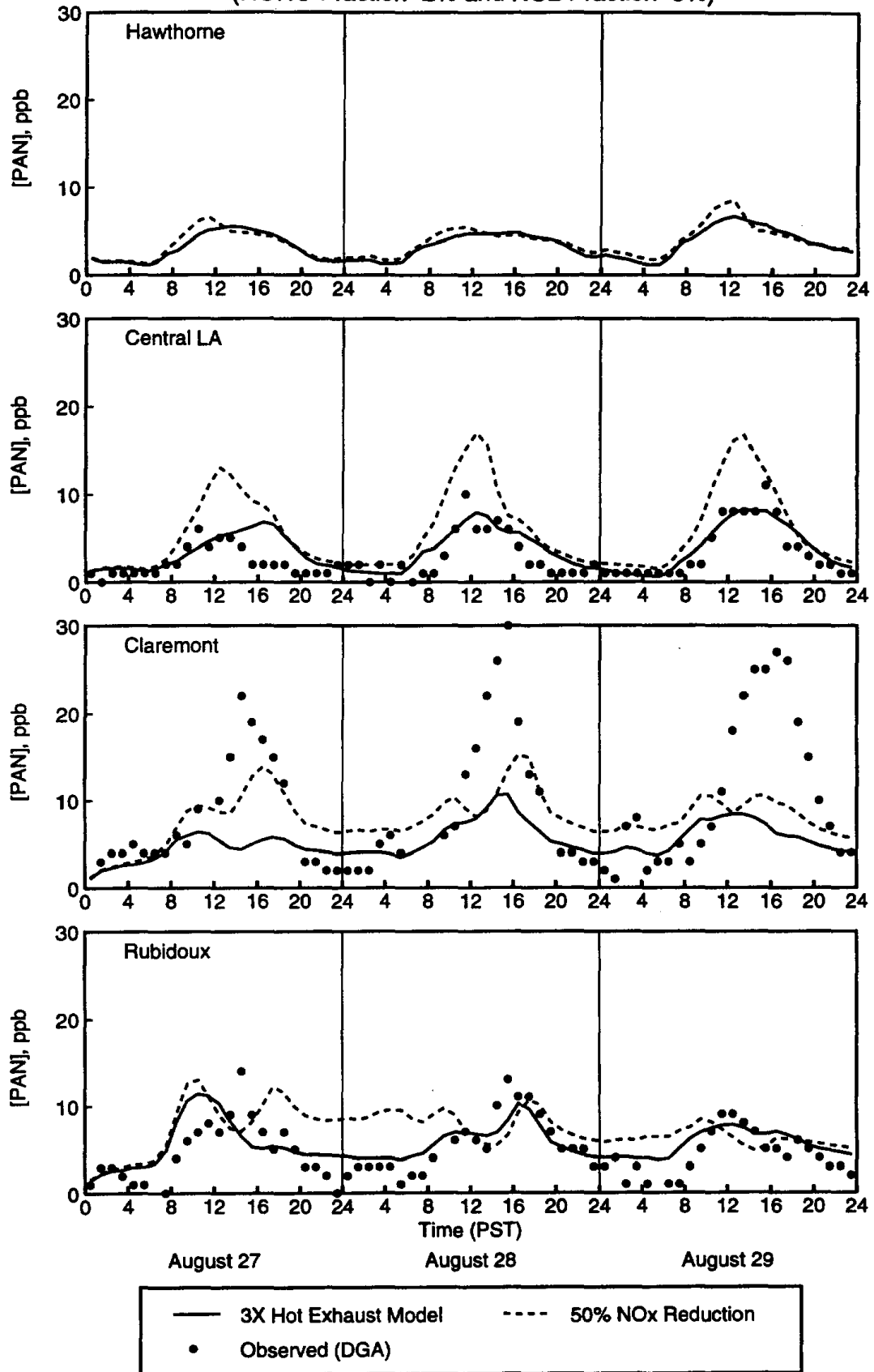
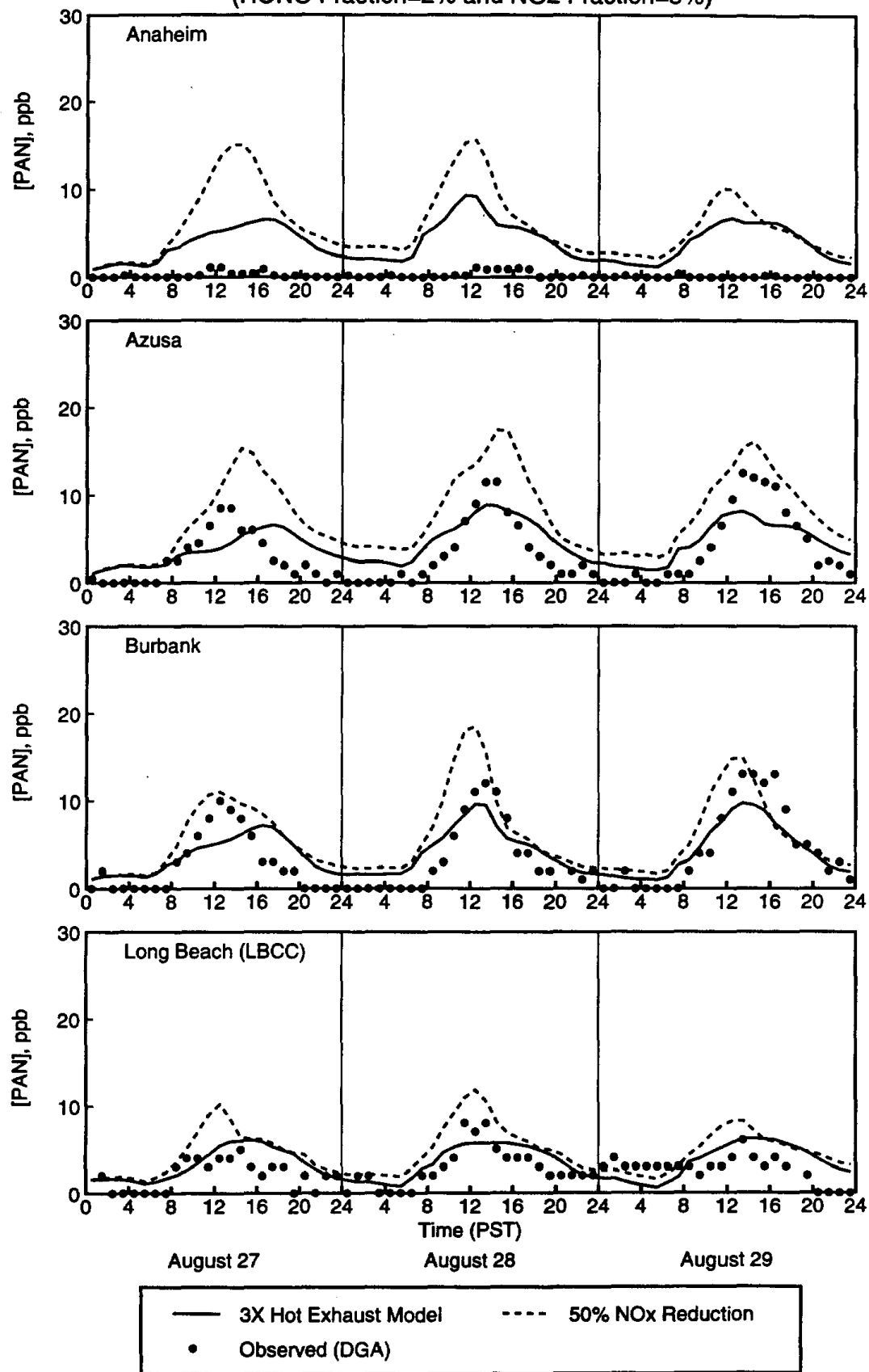


Figure A.9: Peroxyacetyl Nitrate Time Series Plots
(HONO Fraction=2% and NO₂ Fraction=5%)



B Concentration Isopleth Plots

The spatial distribution of predicted pollutant concentrations are shown in a series of isopleth plots that are included in this appendix. Isopleths are plotted for August 28 from 1400-1500 hours PST, a time of peak photochemical activity. Each page that follows contains a matched pair of figures: model predictions using the baseline emission inventory, and predicted concentrations after a 50% cut in NO_x emissions. The figures are presented in the following order:

- B.1 + B.2 Ozone isopleths
- B.3 + B.4 True nitrogen dioxide (NO₂) isopleths
- B.5 + B.6 Nitric acid isopleths
- B.7 + B.8 Fine particle nitrate isopleths
- B.9 + B.10 Peroxyacetyl nitrate isopleths

FIGURE B.1
Predicted Ozone (ppb) using Baseline Emissions

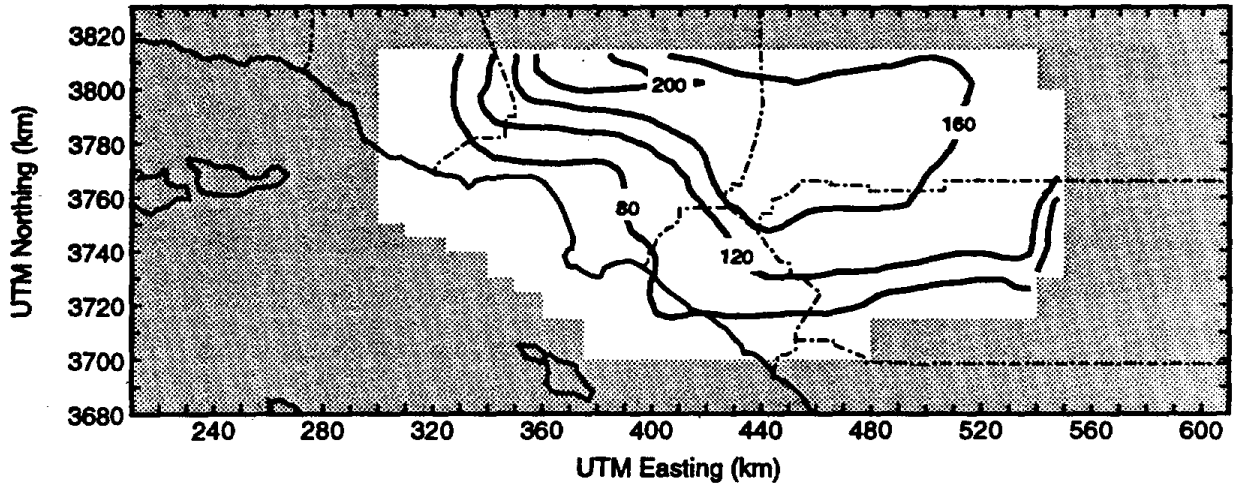


FIGURE B.2
Predicted Ozone (ppb) with 50% Reduction in NO_x Emissions

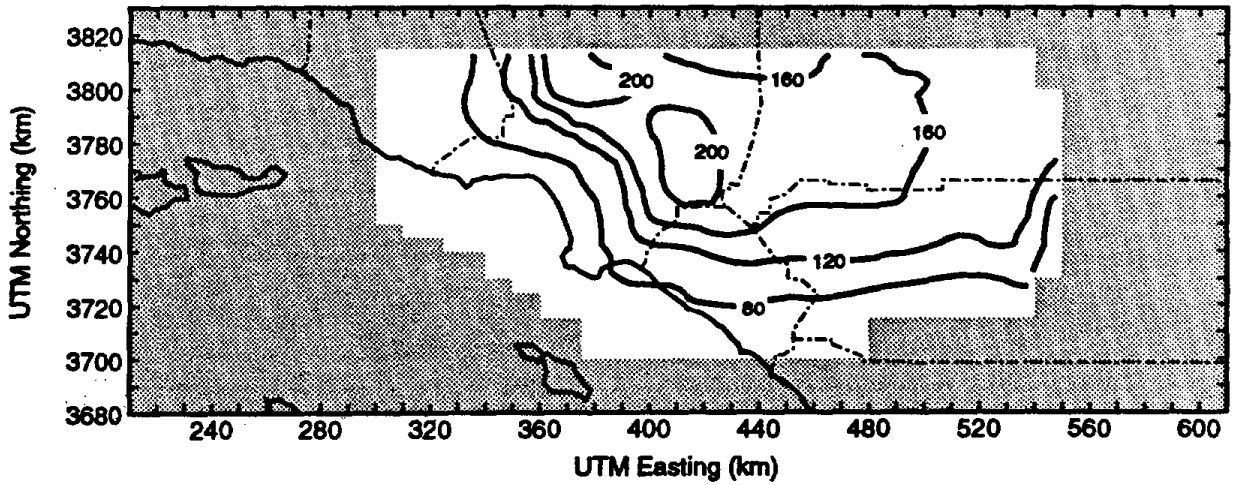


FIGURE B.3
Predicted NO₂ (ppb) using Baseline Emissions

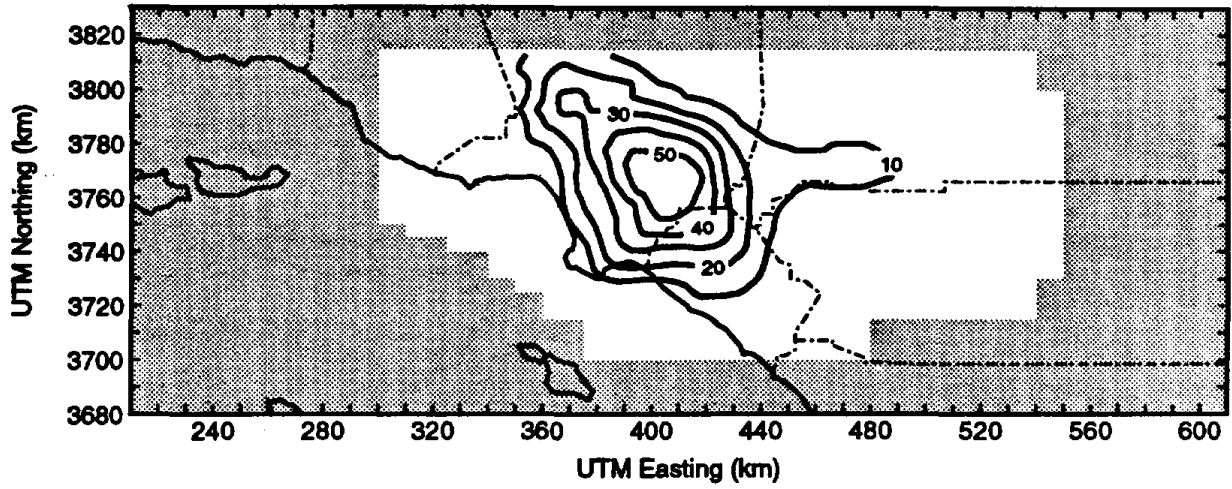


FIGURE B.4
Predicted NO₂ (ppb) with 50% Reduction in NO_x Emissions

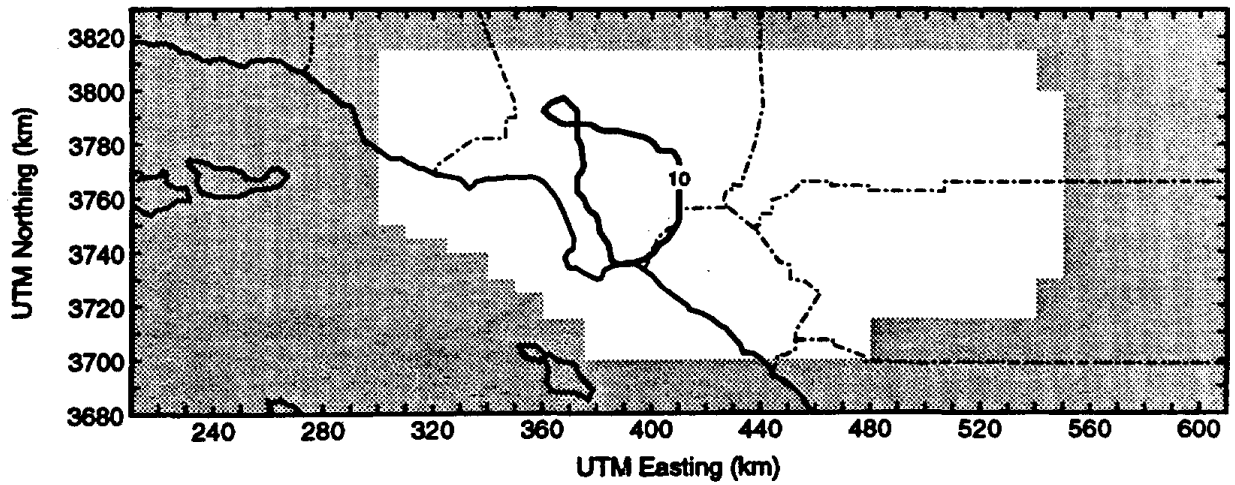


FIGURE B.5
Predicted Nitric Acid (ppb) using Baseline Emissions

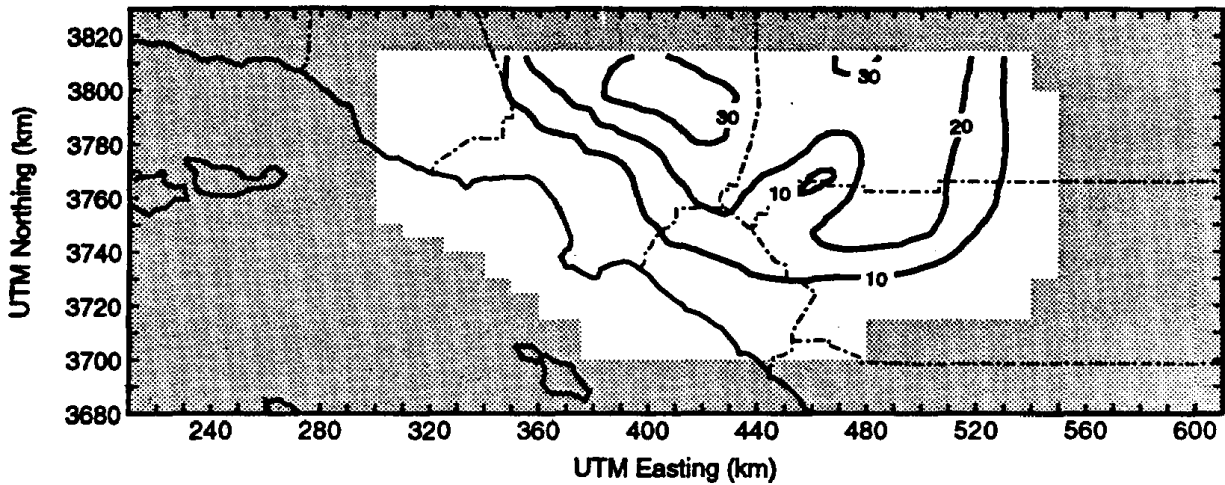


FIGURE B.6
Predicted Nitric Acid (ppb) with 50% Reduction in NO_x Emissions

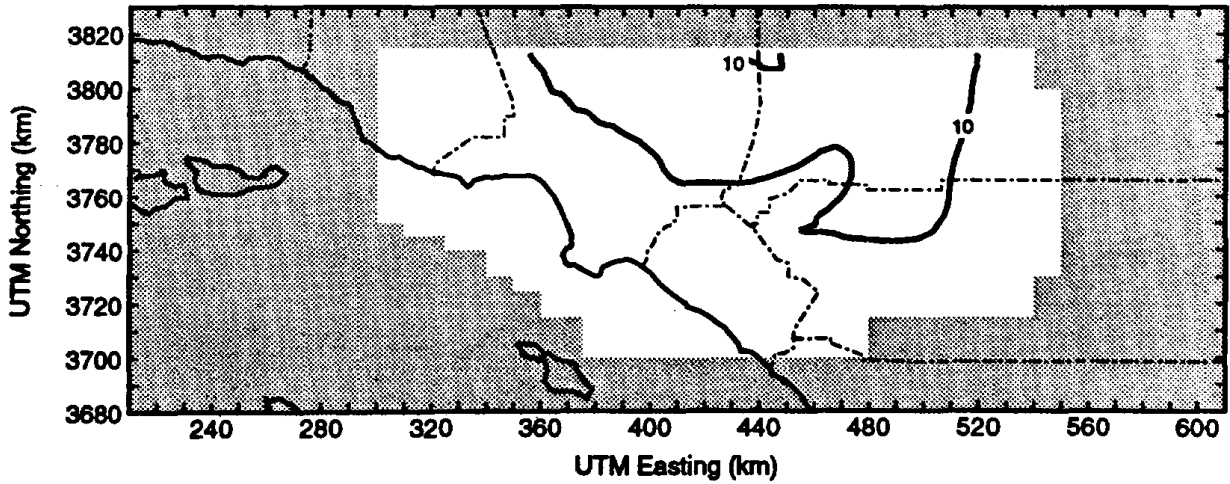


FIGURE B.7
Predicted Fine Particle Nitrate ($\mu\text{g}/\text{m}^3$) using Baseline Emissions

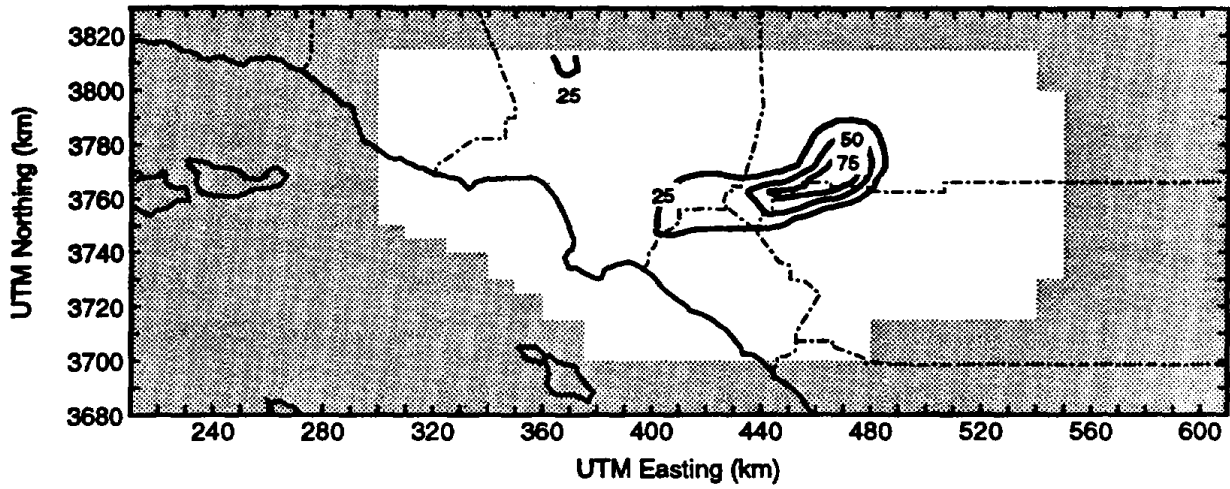


FIGURE B.8
Predicted Fine Particle Nitrate ($\mu\text{g}/\text{m}^3$) with 50% Reduction in NO_x Emissions

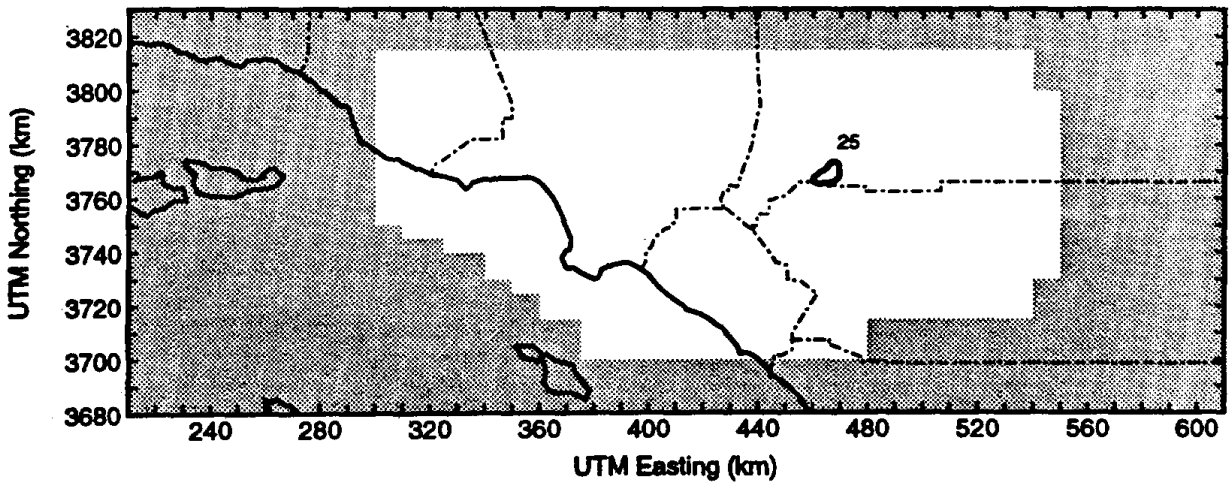


FIGURE B.9
Predicted Peroxyacetyl Nitrate (ppb) using Baseline Emissions

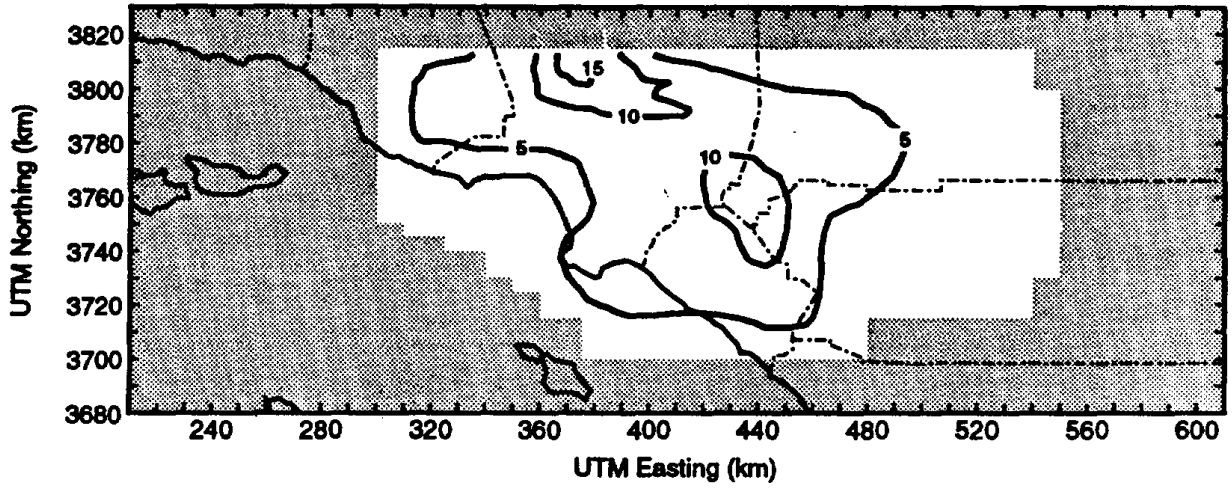
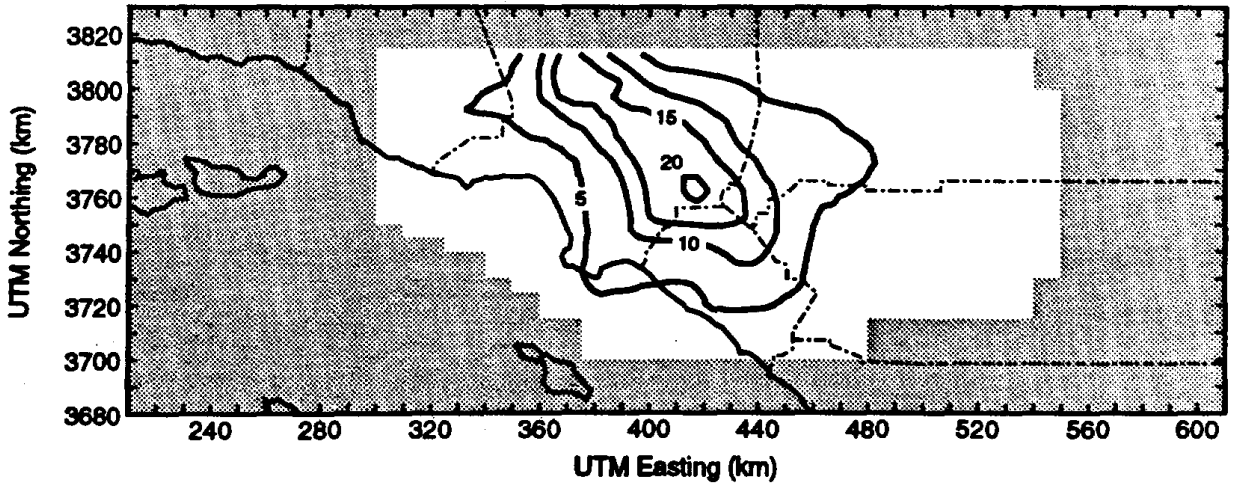


FIGURE B.10
Predicted Peroxyacetyl Nitrate (ppb) with 50% Reduction in NOx Emissions





CARE LIBRARY

10756

REPORT DOCUMENTATION PAGE

1. AGENCY USE ONLY <i>(Leave Blank)</i> PB97-106314		2. REPORT DATE May 1996		3. REPORT TYPE AND DATES COVERED Final Report	
4. TITLE AND SUBTITLE "Impact of Improved Emissions Characterization for Nitrogen-Containing Air Pollutants for the South Coast Air Basin"				5. FUNDING NUMBERS 93-310	
6. AUTHOR(S) Robert A. Harley					
7. PERFORMING ORGANIZATION NAME(S) AND ADDRESS(ES) University of California, Berkeley				8. PERFORMING ORGANIZATION REPORT NUMBER	
9. SPONSORING/MONITORING AGENCY NAME(S) AND ADDRESS(ES) California Air Resources Board Research Division 2020 L Street Sacramento, CA 95814				10. SPONSORING/MONITORING AGENCY REPORT NUMBER ARB/R-96/609	
11. SUPPLEMENTARY NOTES					
12a. DISTRIBUTION/AVAILABILITY STATEMENT Release unlimited. Available from National Technical Information Service. 5285 Port Royal Road Springfield, VA 22161				12b. DISTRIBUTION CODE	
13. ABSTRACT <i>(Maximum 200 Words)</i> <p>The impact of improved characterization of emissions of oxides of nitrogen and ammonia was studied using the CIT airshed model applied to the August 27-29, 1987, intensive monitoring period from the Southern California Air Quality Study. Direct NO₂ and nitrous acid emissions at levels between 0-10% and 0-3%, respectively, were used to examine the influence of NO_x emission speciation. A 50% reduction in total NO_x mass emissions was used to compare the importance of mass emissions and emission speciation.</p> <p>Model predictions matched the spatial and temporal distribution of observed concentrations of O₃, NO₂, PAN, HNO₃, and fine particle nitrate. Predicted pollutant concentrations were much more sensitive to NO_x mass emissions than to NO_x speciation. Daytime NO₂ concentrations were governed by the rate of conversion of NO to NO₂ in the atmosphere, not by direct NO₂ emissions. Nighttime NO₂ and nitrous acid concentrations were sensitive to NO_x speciation. Reducing NO_x emissions led to significant reductions in concentrations of NO₂, nitric acid, and fine particle nitrate, whereas predicted ozone and PAN concentrations increased.</p> <p>To support modeling and control strategy development for nitrogenous air pollutants, improvements are needed to the ammonia emission inventory.</p>					
14. SUBJECT TERMS NO _x , Airshed Model, Air Pollution, Emissions, South Coast Air Basin, Control Strategy, Ammonia.				15. NUMBER OF PAGES	
				16. PRICE CODE PAPER \$21.50	
17. SECURITY CLASSIFICATION OF REPORT Unclassified		18. SECURITY CLASSIFICATION OF THIS PAGE Unclassified		19. SECURITY CLASSIFICATION OF ABSTRACT Unclassified	
				20. LIMITATION OF ABSTRACT Unlimited	

